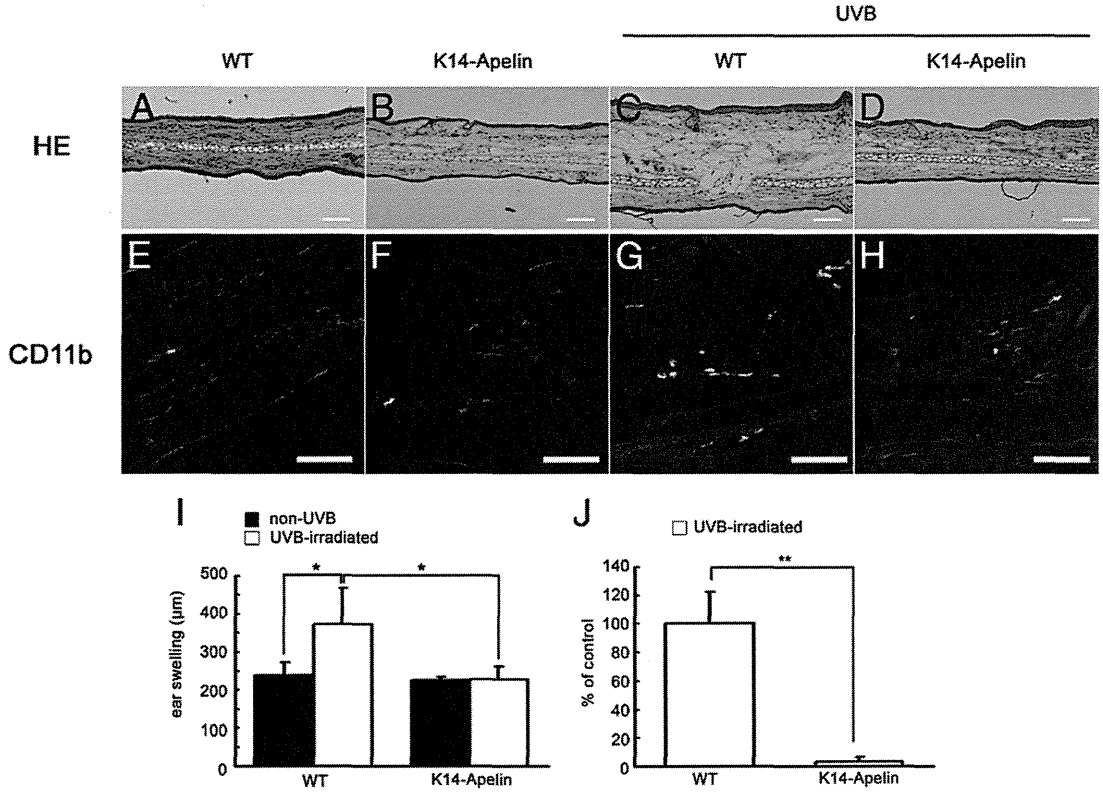

Figure 2. Apelin attenuates UVB-induced edema formation and inflammation. **A–D:** H&E staining revealed marked edema formation in the dermis of WT mouse ear skin (**C**), but K14-apelin mouse ear skin irradiated with UVB (**D**) was similar to non-UVB-irradiated skin (**A** and **B**). Scale bars: 100 μm. **E–H:** Immunofluorescence for CD11b (green) showed decreased macrophage infiltration in the dermis of K14-apelin mice ears (**H**), similar to non-UVB-irradiated mice (**E** and **F**), compared with WT mice irradiated with UVB (**G**). Scale bars: 100 μm. **I:** Skin thickness analysis indicated ear swelling in WT mice after UVB irradiation ($^{*}P < 0.05$), but this swelling was attenuated in K14-apelin mice. $^{*}P < 0.05$. **J:** The number of CD11b-positive cells was decreased in K14-apelin mice after UVB irradiation, compared with UVB-irradiated WT mice. $^{**}P < 0.01$. Morphometric analyses (**I** and **J**) were performed using IP-LAB software version 4.0. Data are expressed as mean values ± SD ($n = 3$).

by UVB irradiation, we analyzed cutaneous lymphatic vessels after UVB irradiation. To visualize lymphatic vessels, Evans Blue dye was injected intradermally into the rim of mouse ears. At 1 and 5 minutes after injection, Evans Blue dye had extravasated from lymphatic vessels in UVB-irradiated WT skin, but such leakage was attenuated in K14-apelin mice (Figure 3, A–D). Next, Miles assay was performed to determine the effects of apelin on blood vessels. UVB exposure induced marked leakage of Evans Blue dye in WT mice (Figure 3E), but such leakage was attenuated in K14-apelin mice (Figure 3F). Quantitative analysis demonstrated that the increase of dye leakage in WT mouse ears was significantly blocked in UVB-irradiated K14-apelin mice (Figure 3G).

We performed double immunofluorescence staining for the lymphatic marker podoplanin and the blood vascular marker Meca-32. In a physiological condition, the density of blood vessels was similar between WT and K14-apelin mice, but K14-apelin mice exhibited increased size of blood vessels, as has been demonstrated previously.[31] No great difference in lymphatic vessel formation was immediately evident in K14-apelin mice; however, precise histological examination of skin stained for podoplanin revealed enlarged lymphatic vessels of K14-apelin mice, compared with WT mice (Figure 3, H–M). Enlargement of lymphatic vessels and blood vessels was induced in WT mice after UVB irradiation; surprisingly, however, in K14-apelin mice the UVB-induced enlargement of lymphatic and blood vessels was inhibited (Figure 3, N–S). Morphometric analyses of sections demonstrated that the average size of lymphatic vessels and blood vessels was significantly decreased in skin of UVB-irradiated K14-apelin mice, compared with WT mice after UVB-irradiation (−74%, $P < 0.05$ for lymphatic vessels; −26%, $P < 0.05$ for blood vessels; Figure 3, T and U).

Discussion

Apelin has been recently reported to be an important regulator of blood vessel formation. The present study reveals, for the first time, that the apelin receptor APJ is expressed by human lymphatic endothelial cells and that apelin/APJ signaling plays a crucial role in UVB-induced inflammation through stabilization of blood and lymphatic vessels.

Acute photodamage of the skin is characterized by epidermal hyperplasia, erythema, and edema formation. Edema is caused by accumulation of extracellular fluid due to excess leakage from hyperpermeable blood vessels[33] and by a failure of lymphatic vessels to sufficiently drain the fluid from the interstitium.[12] Moreover, the dys-

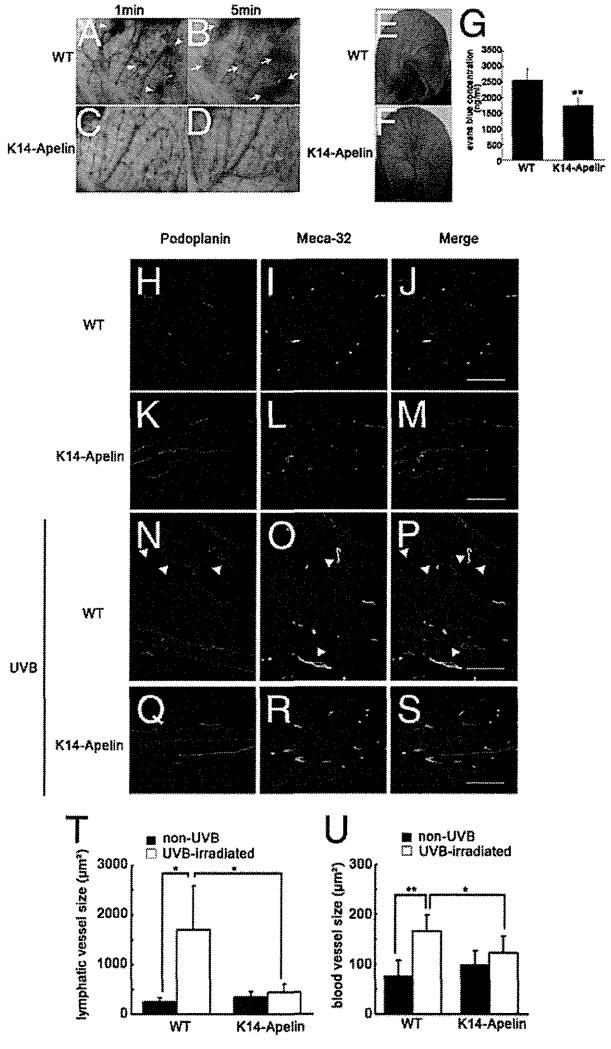

Figure 3. Activation of apelin/APJ signaling inhibited UVB-induced inflammation by blocking enlargement of lymphatic vessels and blood vessels. **A–D:** Evans Blue dye was injected intradermally into the rim of mouse ears. After 5 minutes, Evans Blue dye had extravasated from lymphatic vessels in UVB-irradiated WT mouse skin (**A**, **arrowheads**; **B**, **arrows**), but such leakage was attenuated in K14-apelin mice after UVB (**C** and **D**). **E–G:** Miles assay revealed that UVB exposure induced vascular hyperpermeability of WT mice (**E**), but this effect was markedly inhibited in K14-apelin mice (**F**). **G:** Quantitative analysis demonstrated increased Evans Blue leakage in the ear of UVB-irradiated WT mice, compared with UVB-irradiated K14-apelin mice. $^{**}P < 0.01$. **H–S:** Double immunofluorescence staining of ear sections for podoplanin (red) and Meca-32 (green) revealed enlargement (**arrowheads**) of podoplanin-positive lymphatic vessels and Meca-32-positive blood vessels in UVB-irradiated WT mice (**N–P**), compared with nonirradiated mice (**H–M**). This enlargement of lymphatic vessels and blood vessels after UVB irradiation was blocked in K14-apelin mice (**Q–S**). Scale bars: 100 μm. **T** and **U:** According to morphometric analyses using IP-LAB software version 4.0, the average size of lymphatic vessels (**T**) and blood vessels (**U**) was significantly reduced in K14-apelin mice after UVB irradiation ($^{*}P < 0.05$). In contrast, size of lymphatic vessels and blood vessels was increased in WT mice irradiated with UVB. $^{*}P < 0.05$; $^{**}P < 0.01$.

function of lymphatic vessels also results in reduced clearance of macrophages from the tissue via lymphatic drainage,[34] suggesting that the function of lymphatic vessels is profoundly related to the process of UVB-induced inflammation. We have previously reported that skin tissues during days 2 to 4 after UVB irradiation exhibit enlargement of lymphatic vessels and macrophage infiltration.[13] Surprisingly, K14-apelin mice inhibited the enlargement and hyperpermeability of lymphatic vessels and macrophage infiltration by UVB irradiation, indicating that apelin plays a defensive role in UVB-induced inflammation.

How does apelin attenuate skin inflammation? Although the function of the apelin/APJ system in endothelial cells is known to activate endothelial nitric oxide synthase (eNOS), resulting in decreased the blood pressure with vasodilation,[22] the present results indicate that apelin attenuates the abnormal enlargement of lymphatic and blood vessels in inflamed skin. Additionally, plasma extravasation was markedly decreased in K14-apelin mice, compared with WT mice after UVB irradiation, indicating a protective role of apelin in blood vessels, as described recently.[31] Moreover, we have previously demonstrated that systemic blockade of lymphatic function by the VEGFR-3 pathway prolongs UVB-induced edema formation and inflammation,[35] whereas intradermal injection of VEGF-C accelerates the resolution of UVB-induced edema and inflammation by inducing lymphangiogenesis.[13] In contrast to such VEGF-C treatment, no major differences in the number of lymphatic vessels were observed in skin of K14-apelin mice. It was therefore of considerable interest to see the differential mechanism of attenuating inflammation by apelin. A previous study from our research group demonstrated that acute UVB irradiation increases overextension of lymphatic vessels, which leads to impaired fluid transport and so contributes to prolonged edema formation.[12] Of note, the hyperpermeability of lymphatic vessels was blocked in K14-apelin mice after UVB irradiation, compared with that observed in UVB-irradiated WT mice, and the permeability assay *in vitro* demonstrated that apelin blocked the permeability of human lymphatic endothelial cells. Taken together, these data suggest that inhibiting hyperpermeability by enhancing apelin expression could facilitate transport of tissue fluid, resulting in rapid resolution of edema and the related inflammation induced by UVB.

The molecular events that regulate blood vessel formation, especially the caliber size determination of blood vessels by apelin, have been recently suggested. A remarkable study showed that the apelin/APJ system is involved in downstream signaling of Ang1/Tie2 in blood vessel formation.[26] With the present study, we have demonstrated that apelin induces migration and cord formation of LECs and that lymphatic vascular size in K14-apelin mice is greater than in WT mice. Given that apelin induces expression of the junctional proteins claudin-5 and vascular endothelial cadherin (VE-cadherin) in blood vessels, resulting in abundant cell-to-cell contact and regulation of endothelial cell assembly, it is possible that apelin inhibits hyperpermeability of lymphatic vessels and inflammation by UVB-irradiation via the regulation of the junctional protein in lymphatic endothelial cells.[26] Further studies would be needed to clarify a molecular regulation of lymphatic integrity by apelin and to determine whether apelin is involved in downstream Ang1/Tie2 signaling in lymphatic vessels.

In summary, the present results indicate that apelin plays a functional role in the stabilization of lymphatic vessels in inflamed tissues. Apelin might be a new

suitable target for prevention of UVB-induced skin inflammation.

Acknowledgment

We thank Fumika Miyohashi for her technical assistance.

References

1. Cueni LN, Detmar M: New insights into the molecular control of the lymphatic vascular system and its role in disease. J Invest Dermatol 2006, 126:2167–2177
2. Tammela T, Alitalo K: Lymphangiogenesis: molecular mechanisms and future promise. Cell 2010, 140:460–476
3. Kunstfeld R, Hirakawa S, Hong YK, Schacht V, Lange-Asschenfeldt B, Velasco P, Lin C, Fiebiger E, Wei X, Wu Y, Hicklin D, Bohlen P, Detmar M: Induction of cutaneous delayed-type hypersensitivity reactions in VEGF-A transgenic mice results in chronic skin inflammation associated with persistent lymphatic hyperplasia. Blood 2004, 104:1048–1057
4. Kligman AM: The treatment of photoaged human skin by topical tretinoin. Drugs 1989, 38:1–8
5. Kripke ML: Ultraviolet radiation and immunology: something new under the sun—presidential address. Cancer Res 1994, 54:6102–6105
6. Yano K, Kadoya K, Kajiya K, Hong YK, Detmar M: Ultraviolet B irradiation of human skin induces an angiogenic switch that is mediated by upregulation of vascular endothelial growth factor and by downregulation of thrombospondin-1. Br J Dermatol 2005, 152:115–121
7. Yano K, Kajiya K, Ishiwata M, Hong YK, Miyakawa T, Detmar M: Ultraviolet B-induced skin angiogenesis is associated with a switch in the balance of vascular endothelial growth factor and thrombospondin-1 expression. J Invest Dermatol 2004, 122:201–208
8. Krämer M, Sachsenmaier C, Herrlich P, Rahmsdorf HJ: UV irradiation-induced interleukin-1 and basic fibroblast growth factor synthesis and release mediate part of the UV response. J Biol Chem 1993, 268: 6734–6741
9. Strickland I, Rhodes LE, Flanagan BF, Friedmann PS: TNF-alpha and IL-8 are upregulated in the epidermis of normal human skin after UVB exposure: correlation with neutrophil accumulation and E-selectin expression. J Invest Dermatol 1997, 108:763–768
10. Hirakawa S, Fujii S, Kajiya K, Yano K, Detmar M: Vascular endothelial growth factor promotes sensitivity to ultraviolet B-induced cutaneous photodamage. Blood 2005, 105:2392–2399
11. Yano K, Oura H, Detmar M: Targeted overexpression of the angiogenesis inhibitor thrombospondin-1 in the epidermis of transgenic mice prevents ultraviolet-B-induced angiogenesis and cutaneous photo-damage. J Invest Dermatol 2002, 118:800–805
12. Kajiya K, Hirakawa S, Detmar M: Vascular endothelial growth factor-a mediates ultraviolet B-induced impairment of lymphatic vessel function. Am J Pathol 2006, 169:1496–1503
13. Kajiya K, Sawane M, Huggenberger R, Detmar M: Activation of the VEGFR-3 pathway by VEGF-C attenuates UVB-induced edema formation and skin inflammation by promoting lymphangiogenesis. J Invest Dermatol 2009, 129:1292–1298
14. Hosoya M, Kawamata Y, Fukusumi S, Fujii R, Habata Y, Hinuma S, Kitada C, Honda S, Kurokawa T, Onda H, Nishimura O, Fujino M: Molecular and functional characteristics of APJ. Tissue distribution of mRNA and interaction with the endogenous ligand apelin. J Biol Chem 2000, 275:21061–21067
15. Tatemoto K, Hosoya M, Habata Y, Fujii R, Kakegawa T, Zou MX, Kawamata Y, Fukusumi S, Hinuma S, Kitada C, Kurokawa T, Onda H, Fujino M: Isolation and characterization of a novel endogenous peptide ligand for the human APJ receptor. Biochem Biophys Res Commun 1998, 251:471–476
16. Masri B, Knibiehler B, Audigier Y: Apelin signalling: a promising pathway from cloning to pharmacology. Cell Signal 2005, 17:415–426
17. Devic E, Rizzoti K, Bodin S, Knibiehler B, Audigier Y: Amino acid sequence and embryonic expression of msr/apj, the mouse homolog of Xenopus X-msr and human APJ. Mech Dev 1999, 84:199–203
18. O'Dowd BF, Heiber M, Chan A, Heng HH, Tsui LC, Kennedy JL, Shi X, Petronis A, George SR, Nguyen T: A human gene that shows identity with the gene encoding the angiotensin receptor is located on chromosome 11. Gene 1993, 136:355–360
19. De Mota N, Reaux-Le Goazigo A, El Messari S, Chartrel N, Roesch D, Dujardin C, Kordon C, Vaudry H, Moos F, Llorens-Cortes C: Apelin, a potent diuretic neuropeptide counteracting vasopressin actions through inhibition of vasopressin neuron activity and vasopressin release. Proc Natl Acad Sci USA 2004, 101:10464–10469
20. Devic E, Paquereau L, Vernier P, Knibiehler B, Audigier Y: Expression of a new G protein-coupled receptor X-msr is associated with an endothelial lineage in Xenopus laevis. Mech Dev 1996, 59:129–140
21. Katugampola SD, Maguire JJ, Matthewson SR, Davenport AP: [(125)I]-(Pyr(1))Apelin-13 is a novel radioligand for localizing the APJ orphan receptor in human and rat tissues with evidence for a vasoconstrictor role in man. Br J Pharmacol 2001, 132:1255–1260
22. Ishida J, Hashimoto T, Hashimoto Y, Nishiwaki S, Iguchi T, Harada S, Sugaya T, Matsuzaki H, Yamamoto R, Shiota N, Okunishi H, Kihara M, Umemura S, Sugiyama F, Yagami K, Kasuya Y, Mochizuki N, Fukamizu A: Regulatory roles for APJ, a seven-transmembrane receptor related to angiotensin-type 1 receptor in blood pressure in vivo. J Biol Chem 2004, 279:26274–26279
23. Tatemoto K, Takayama K, Zou MX, Kumaki I, Zhang W, Kumano K, Fujimiya M: The novel peptide apelin lowers blood pressure via a nitric oxide-dependent mechanism. Regul Pept 2001, 99:87–92
24. Cox CM, D'Agostino SL, Miller MK, Heimark RL, Krieg PA: Apelin, the ligand for the endothelial G-protein-coupled receptor, APJ, is a potent angiogenic factor required for normal vascular development of the frog embryo. Dev Biol 2006, 296:177–189
25. Scott IC, Masri B, D'Amico LA, Jin SW, Jungblut B, Wehman AM, Baier H, Audigier Y, Stainier DY: The G protein-coupled receptor Agtrl1b regulates early development of myocardial progenitors. Dev Cell 2007, 12:403–413
26. Kidoya H, Ueno M, Yamada Y, Mochizuki N, Nakata M, Yano T, Fujii R, Takakura N: Spatial and temporal role of the apelin/APJ system in the caliber size regulation of blood vessels during angiogenesis. EMBO J 2008, 27:522–534
27. Hirakawa S, Hong YK, Harvey N, Schacht V, Matsuda K, Libermann T, Detmar M: Identification of vascular lineage-specific genes by transcriptional profiling of isolated blood vascular and lymphatic endothelial cells. Am J Pathol 2003, 162:575–586
28. Kajiya K, Hirakawa S, Ma B, Drinnenberg I, Detmar M: Hepatocyte growth factor promotes lymphatic vessel formation and function. EMBO J 2005, 24:2885–2895
29. Hong YK, Lange-Asschenfeldt B, Velasco P, Hirakawa S, Kunstfeld R, Brown LF, Bohlen P, Senger DR, Detmar M: VEGF-A promotes tissue repair-associated lymphatic vessel formation via VEGFR-2 and the alpha1beta1 and alpha2beta1 integrins. FASEB J 2004, 18:1111–1113
30. Kajiya K, Huggenberger R, Drinnenberg I, Ma B, Detmar M: Nitric oxide mediates lymphatic vessel activation via soluble guanylate cyclase alpha1beta1: impact on inflammation. FASEB J 2008, 22: 530–537
31. Kidoya H, Naito H, Takakura N: Apelin induces enlarged and nonleaky blood vessels for functional recovery from ischemia. Blood 2010, 115:3166–3174
32. Masri B, Morin N, Pedebernade L, Knibiehler B, Audigier Y: The apelin receptor is coupled to Gi1 or Gi2 protein and is differentially desensitized by apelin fragments. J Biol Chem 2006, 281:18317–18326
33. Persson CG: Role of plasma exudation in asthmatic airways. Lancet 1986, 2:1126–1129
34. Kataru RP, Jung K, Jang C, Yang H, Schwendener RA, Baik JE, Han SH, Alitalo K, Koh GY: Critical role of CD11b+ macrophages and VEGF in inflammatory lymphangiogenesis, antigen clearance, and inflammation resolution. Blood 2009, 113:5650–5659
35. Kajiya K, Detmar M: An important role of lymphatic vessels in the control of UVB-induced edema formation and inflammation. J Invest Dermatol 2006, 126:919–921

Biochemical and Biophysical Research Communications 415 (2011) 174–180

Contents lists available at SciVerse ScienceDirect

Biochemical and Biophysical Research Communications

journal homepage: www.elsevier.com/locate/ybbrc

2-Methoxycinnamaldehyde inhibits tumor angiogenesis by suppressing Tie2 activation

Daishi Yamakawa [a], Hiroyasu Kidoya [a], Susumu Sakimoto [a], Weizhen Jia [a], Nobuyuki Takakura [a,b,*]

[a] Department of Signal Transduction, Research Institute for Microbial Diseases, Osaka University, 3-1 Yamada-oka, Suita-shi, Osaka 565-0871, Japan
[b] JST, CREST, Sanbancho, Chiyoda-ku, Tokyo 102-0075, Japan

ARTICLE INFO

Article history:
Received 20 September 2011
Available online 18 October 2011

Keywords:
2-Methoxycinnamaldehyde
Tie2
Angiopoietin-1
Angiogenesis

ABSTRACT

Blood vessels are mainly composed of intraluminal endothelial cells (ECs) and mural cells adhering to the ECs on their basal side. Immature blood vessels lacking mural cells are leaky; thus, the process of mural cell adhesion to ECs is indispensable for stability of the vessels during physiological angiogenesis. However, in the tumor microenvironment, although some blood vessels are well-matured, the majority is immature. Because mural cell adhesion to ECs also has a marked anti-apoptotic effect, angiogenesis inhibitors that destroy immature blood vessels may not affect mature vessels showing more resistance to apoptosis. Activation of Tie2 receptor tyrosine kinase expressed in ECs mediates pro-angiogenic effects via the induction of EC migration but also facilitates vessel maturation via the promotion of cell adhesion between mural cells and ECs. Therefore, inhibition of Tie2 has the advantage of completely inhibiting angiogenesis. Here, we isolated a novel small molecule Tie2 kinase inhibitor, identified as 2-methoxycinnamaldehyde (2-MCA). We found that 2-MCA inhibits both sprouting angiogenesis and maturation of blood vessels, resulting in inhibition of tumor growth. Our results suggest a potent clinical benefit of disrupting these two using Tie2 inhibitors.

1. Introduction

It is well-established that dysregulation of blood vessel formation is involved in several diseases, such as cancer, retinopathy, chronic inflammation and others. To develop optimal strategies for inhibiting angiogenesis and preventing progression of these diseases, the mechanisms controlling blood vessel formation have been extensively analyzed. Of the many growth factors involved in this process, vascular endothelial growth factor (VEGF) or its cognate receptors (VEGFRs) have been targeted by angiogenesis inhibitors which are already utilized clinically, especially in cancer therapy [1]. Indeed, the efficacy of neutralizing antibody to VEGF (bevacizumab) in prolonging survival in patients with malignant colon cancer has been established, and utilization of this drug is currently being extended to other tumor types [2].

VEGF plays a fundamental role in development, tube formation and proliferation of endothelial cells (ECs) [3]. Tubes generated using VEGF alone do not mature; blood vessel stability requires the adherence of mural cells such as pericytes or smooth muscle cells to ECs on the basal side. When Tie2, a receptor tyrosine kinase, expressed predominantly in ECs, is activated by angiopoietin-1 (Ang1), usually released from mural cells, cell adhesion between ECs and mural cells is induced and the structural stability of blood vessels is enhanced [4]. It is widely accepted that mural cell adhesion to ECs induces a transition from the actively elongating status of a new blood vessel to a mature state, resulting in finalization of sprouting angiogenesis. On the other hand, when angiogenesis is ongoing and mural cells are absent near ECs, Tie2 activation induces migration of ECs to support sprouting angiogenesis. Therefore, Tie2 activation plays dual roles as a pro-angiogenic and as an anti-angiogenic factor. Which activity dominates is dependent on intracellular signaling via Tie2 phosphorylation [5]. When it is mainly the Akt pathway that is activated through Tie2, cell adhesion between mural cells and ECs is induced, resulting in vascular quiescence. However, when the Erk rather than Akt pathway is activated via Tie2, the migration of ECs is enhanced.

In the context of therapy with angiogenesis inhibitors, maturation of blood vessels is a key locus for the development of resistance against angiogenesis inhibitors. Mural cells adhere to ECs in mature blood vessels. In this situation, the two cell types engage in cross-talk and stimulate each other by producing several cytokines such as VEGF, Ang1, platelet-derived growth factor (PDGF), transforming growth factor β and others [6]. This results in suppression of apoptosis of both mural cells and ECs. Moreover,

Abbreviations: 2-MCA, 2-methoxycinnamaldehyde; EC, endothelial cell; Ang1, angiopoietin-1; VEGF, vascular endothelial growth factor.

* Corresponding author at: Department of Signal Transduction, Research Institute for Microbial Diseases, Osaka University, 3-1 Yamada-oka, Suita-shi, Osaka 565-0871, Japan. Fax: +81 6879 8314.
E-mail address: ntakaku@biken.osaka-u.ac.jp (N. Takakura).

0006-291X/$ - see front matter © 2011 Elsevier Inc. All rights reserved.
doi:10.1016/j.bbrc.2011.10.053

adhesion molecules responsible for keeping the mural cells and ECs in close proximity also provide signals involved in preventing their apoptosis. Tie2- or Ang1-deficient mice lack EC/mural cell integrity and manifest insufficient vessel outgrowth [7]. Therefore, Tie2 inhibition in tumors may suppress sprouting angiogenesis as well as inhibiting blood vessel maturation.

In the present study, we screened for small molecule Tie2 inhibitors in natural products. Among the molecules investigated, we found that 2-methoxycinnamaldehyde [(2E)-3-(2-methoxyphenyl)acrylaldehyde: 2-MCA] inhibits Ang1-mediated Tie2 phosphorylation. 2-MCA is extracted from the bark of cinnamon trees and other species of the genus *Cinnamomum* and gives those plants their flavor [8]. 2-MCA has been identified as the major active fungitoxic component, especially against Candida albicans [9], and also possesses strong antibacterial activity [10]. Here, we show that 2-MCA abrogates Ang1-mediated endothelial barrier function and tube formation in vitro. Moreover, using 2-MCA we analyzed whether Tie2 inhibition suppresses both the process of sprouting angiogenesis as well as blood vessel maturation in the tumor microenvironment.

2. Materials and methods

2.1. Screen for Tie2 kinase inhibitors

Human Tie2, cytoplasmic domain [771-1124(end) aminoacids was expressed as an N-terminal GST-fusion protein. First, we selected extracts from several herbs because of their inhibitory effects on proliferation or migration of ECs in the P-Sp culture system that supports vasculogenesis and angiogenesis [11]. Approximately 100 test compounds were isolated from extracts of these herbs by high performance liquid chromatography were evaluated. Compound solution, substrate/ATP/Metal solution, and kinase solution were prepared with assay buffer (15 mM Tris–HCl, 0.01% Tween-20, 2 mM DTT, pH 7.5) and mixed in streptavidin coated 96 well microplates (Perkin Elmer). Plates were incubated for 1 h at room temperature and then washed four times to stop the reaction. Wells were blocked with blocking buffer containing 0.1% BSA and then the detection antibody (HRP-conjugated PY20; Santa Cruz Biotechnology) was added and incubated for 30 min. After washing, TMB solution (MOSS, Inc.) was added to each well and incubated for 5 min. To stop the HRP reaction, 0.1 M sulfuric acid was added. The kinase reaction was evaluated by absorbance at 450 nm. Among compounds tested, we found one with Tie2 kinase inhibitory effects. This compound was identified as 2-MCA by NMR (NM-ECP400; JOEL).

2.2. Reagents

2-MCA (Sigma Aldrich), Recombinant human $VEGF_{165}$ (PEPROTECH), Ang1, and HGF (R&D Systems) were used.

In Western blotting analysis, mouse anti-Tie2 (Ab33) antibodies (Abs) (Upstate), phospho-Tie2 (Tyr992) (R&D Systems, Inc.), rabbit anti-Akt, phospho-Akt (Ser473), p44/42, phospho-p44/42 (Thr202/Tyr204) (Cell Signaling Technology, Inc.) and mouse anti-GAPDH mAb (Chemicon) were used as the first Abs. Anti-phosphoTie2 (Tyr992) Abs were diluted 1:500, other Abs 1:1000. HRP-conjugated anti-rabbit and anti-mouse Ig (Jackson ImmunoResearch) was used as the secondary antibody (diluted 1:1000).

For the immunofluorescence analysis, mouse anti-human ZO-1 (BD Biosciences), rat anti-mouse CD31 (BD Biosciences) and Cy3-conjugated anti-α-smooth muscle actin (1A4; Sigma) mAbs were used as the first Abs (diluted 1:200). Alexa488-conjugated goat anti-mouse and anti-rat Igs (Invitrogen) were used as the secondary Abs (Invitrogen) (dilution; 1:200).

2.3. Cell culture

Ba/F3 cells were grown in RPMI-1640 medium supplemented with 10% FBS and 200 pg/ml IL-3 (GIBCO). Human umbilical vein endothelial cells (HUVECs) were purchased from Kurabo (Kurashiki, Japan) and maintained according to the supplier's instructions. For Ang1, VEGF and HGF stimulation, cells were starved in RPMI-1640 medium containing 1% FBS for 3 h. Colon26 cells were grown in Dulbecco's modified Eagle's medium (DMEM) supplemented with 10% FBS. HCT116 cells were grown in RPMI-1640 medium supplemented with 10% FBS. Platinum-E cells (Plat-E; packaging cells) and stable cell lines transfected with pMRX virus vector were cultured in 10% FBS-containing DMEM [12,13].

2.4. Plasmid construction

Mouse Tie2 or mutant Tie2 (Tie2R848W) was fused to sequences encoding full-length Venus. A Myc epitope was inserted as a tag between Tie2 and Venus. Genes were inserted at the multicloning site of pEGFPN1 vector or pMRX virus vectors.

2.5. Retroviral infection

Plat-E cells were transfected with 1.0 μg of pMRX-Tie2-Myc-Venus or pMRX-Tie2R848W-Myc-Venus vectors using Lipofectamine 2000 (Invitrogen), then incubated for 24 h at 37 °C after which the medium was changed. After 12 h (36 h from transfection) and 24 h (48 h from transfection), conditioned medium was harvested, sterilized by filtration and used to infect Ba/F3 cells. About 8 μg/ml polybrene was added to facilitate infection. Stable cell lines expressing wild-type Tie2 (BaF/WT-Tie2 cells) or constitutively active Tie2 (BaF/R848W-Tie2 cells) were selected by culture in medium containing puromycin (5 μg/ml) or blasticidin (10 μg/ml).

2.6. SDS–PAGE and Western blotting

Cells were washed with ice-cold phosphate-buffered saline (PBS) and lyzed with RIPA buffer (50 mM Tris–HCl pH 7.5, 150 mM NaCl, 1% NP-40, 0.5% sodium deoxycholate, 0.1% SDS). The cells were incubated on ice for 10 min followed by centrifugation at 15,000 rpm for 5 min at 4 °C. Proteins electrophoretically separated using 7.5% SDS gels were transferred to nylon membranes (Amersham Biosciences) by a wet blotting procedure (140 V, 200 mA, 120 min). The membrane was blocked with 5% skim milk/TBST for 60 min, subsequently incubated with the Abs as indicated in the figures and processed for chemiluminescence detection with ECL solution.

2.7. Tube formation

HUVECs were cultured at 3×10^4 cells/well on 100 μl of growth factor-reduced Matrigel (BD Biosciences) in RPMI-1640 supplemented with 1% FBS. The cells were incubated for 18 h at 37 °C, 5% CO_2. Tube formation was observed in living cells microscopically (Leica AF6000).

2.8. Analysis of cell apoptosis

HUVECs were cultured for 24 h in the presence or absence of 2-MCA (30 μM). The cells were stained with Annexin V and propidium iodide using an Annexin V-FITC apoptosis detection kit (BD Biosciences), and analyzed by flow cytometry (Becton Dickinson).

2.9. Mice

Balb/c and KSN nude mice were purchased from Japan SLC (Shizuoka, Japan). Mouse and human colon cancer-derived colon26 and HCT116 cells (3.5×10^6 cells) were inoculated subcutaneously into 8 week-old female mice. Animals were housed in environmentally controlled rooms of the animal experimentation facility at Osaka University. All experiments were carried out following the guidelines of Osaka University Committee for animal and recombinant DNA experiments.

2.10. Immunocytochemistry and immunohistochemistry

For immunocytochemistry, cells on 0.1% gelatin (Sigma Aldrich)-coated glass dishes were rinsed, fixed for 10 min in 4% paraformaldehyde-PBS (pH 7.5) and washed with PBS. Subsequently, the cells were permeabilized with 0.1% Triton X-100 for 30 min. After washing with PBS, cells were blocked with PBS containing 5% normal goat serum and 1% BSA for 30 min and immunostained with first Abs (1:100) for 1 h. Protein reacting with Abs was visualized with secondary Abs (1:200). The cells were observed under a microscope (Leica TCS SP5 Ver1.6) using HCX PL APO lambda blue 63×1.4 oil. Images were processed using Adobe Photoshop CS5 Extended software (Adobe Systems). Immunohistochemical analysis was performed as previously reported [14].

2.11. Statistical analysis

Results were expressed as the mean ± SEM. Student's t test was used for statistical analysis. Differences were considered statistically significant when $P < 0.01$.

3. Results

3.1. 2-MCA inhibits phosphorylation of Tie2

Using an ELISA-based in vitro kinase assay to screen for Tie2 inhibitors, we identified 2-MCA as a novel candidate molecule. To confirm that 2-MCA inhibits Ang1-mediated Tie2 phosphorylation, a pro-B lymphocyte cell line (Ba/F3) expressing mouse Tie2 ectopically (BaF/WT-Tie2 cells) was used. When BaF/WT-Tie2 cells were stimulated with Ang1, phosphorylation of Tie2 was observed; this was suppressed by 2-MCA in a dose-dependent manner (Fig. 1A).

It is well known that Tie2 phosphorylation induces activation of downstream signal pathways such as PI3K-Akt and p42/44, Erk. We found that 2-MCA inhibited both of these Ang-1-stimulated, Tie2-dependent signaling cascades (Fig. 1B).

It has been reported that exchange of tryptophan for arginine at position 849 (R849W) of Tie2 by point mutation leads to its constitutive activation and that this mutation is one cause of human hereditary venous malformation [15]. We generated a construct

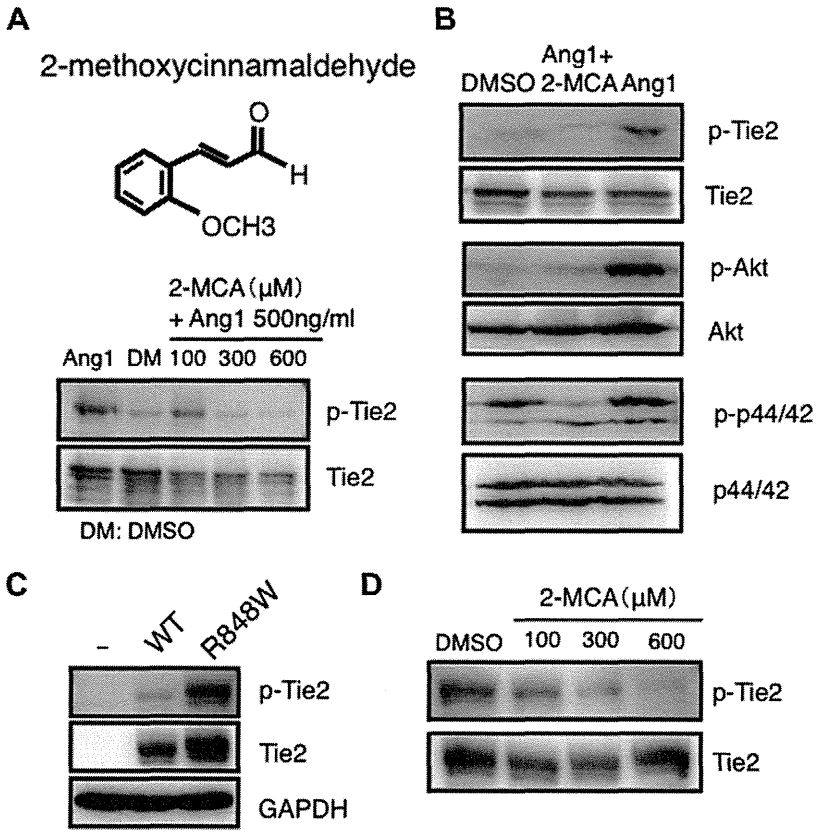

Fig. 1. 2-MCA inhibits phosphorylation of Tie2. (A) Chemical structural formula of 2-methoxycinnamaldehyde (2-MCA) (upper). Western blotting was performed using BaF/WT-Tie2 cells (bottom). BaF/WT-Tie2 cells were stimulated with or without Ang1 for 15 min in the presence or absence of titrated doses of 2-MCA. (B) Effect of 2-MCA on downstream signals of Tie2. BaF/WT-Tie2 cells were stimulated with or without Ang1 (500 ng/ml) for 15 min in the presence or absence of 2-MCA (600 μM). Phosphorylation of Tie2, Akt and p44/42 was assessed. (C) Western blotting of Ba/F3, BaF/WT-Tie2 (WT), and BaF/R848W-Tie2 cells (R848W). GAPDH was used as the internal control. (D) Inhibitory effect of 2-MCA on phosphorylation of constitutively active Tie2. BaF/R848W-Tie2 cells were cultured with titrated doses of 2-MCA as indicated for 15 min. Tie2 phosphorylation was then assessed.

coding for this mutant Tie2 in mice (R848W) and transfected it into Ba/F3 cells. Wild-type Tie2 was only weakly phosphorylated without Ang1 on overexpression, but mutant Tie2 was strongly phosphorylated (Fig. 1C). This phosphorylation of constitutively active Tie2 was also inhibited by 2-MCA in a dose-dependent manner (Fig. 1D).

3.2. 2-MCA inhibits Ang1-mediated stabilization of cell-cell junctions and tube formation

Activation of Tie2 in ECs enhances the stability of blood vessels and supports angiogenesis mainly via Akt or Erk activation, respectively, as described above [5]. Therefore, we next investigated whether 2-MCA affects these functions of Tie2 using human umbilical vein endothelial cells (HUVECs). We confirmed that activation of Akt and Erk mediated by stimulation with Ang1 was abrogated by 2-MCA in HUVECs (Fig. 2A), as was observed using BaF/Tie2 cells. When HUVECs reach confluence, tight junctions marked by ZO-1 appear (Fig. 2B). ZO-1 expression was not observed on EC–EC contact on stimulation with VEGF, consistent with its well known action to disturb EC–EC junction formation and facilitate hyperpermeability [16]. However, Ang1 inhibited VEGF-mediated disruption of junction formation. When 2-MCA was added at the same time as VEGF and Ang1, the effect of Ang1 on stabilization of EC-EC contact was annulled (Fig. 2B). This finding suggested that 2-MCA blocks maturation processes during blood vessel formation. When HUVECs were cultured on the Matrigels, Ang1 was seen to induce cord-like structures involved in tube formation, as previously reported [17] (Fig. 2C). However, 2-MCA suppressed this, consistent with its inhibitory effects on angiogenesis.

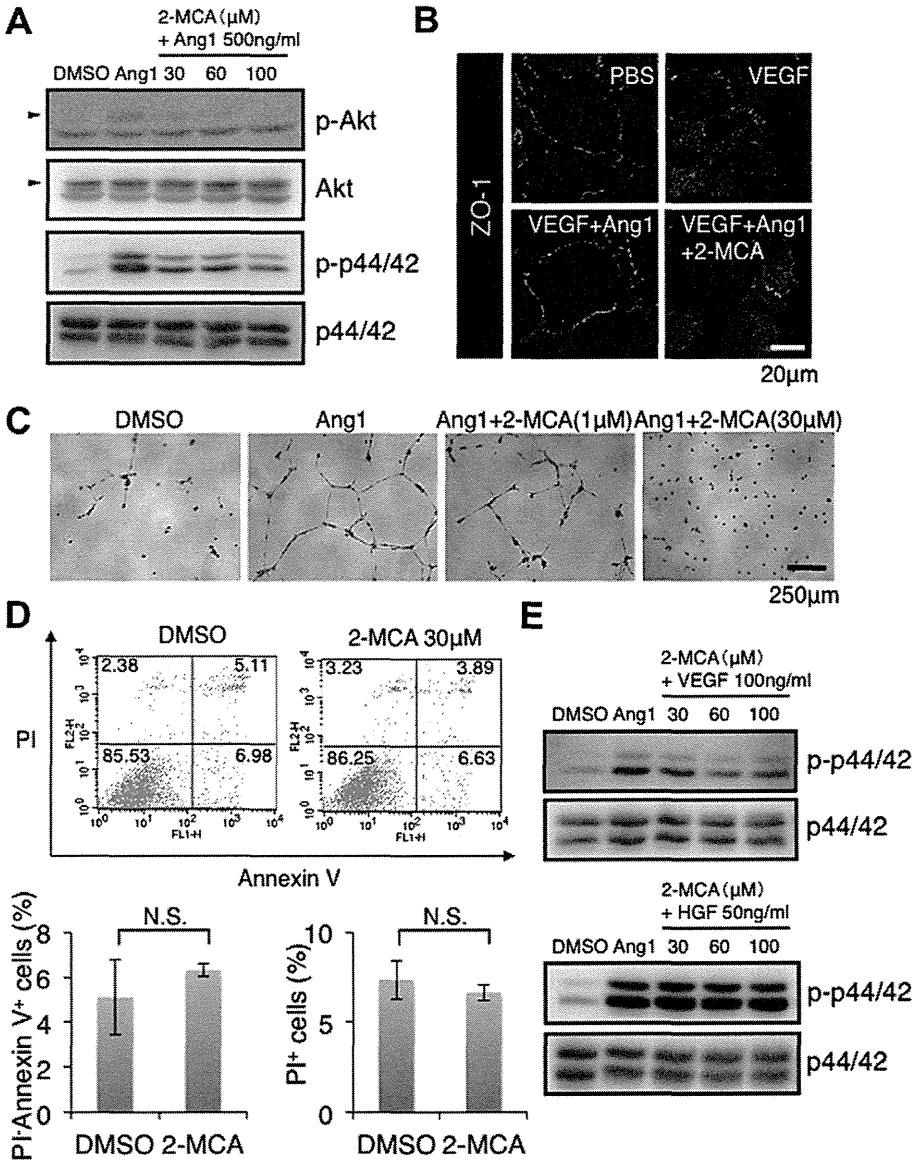

Fig. 2. Effects of 2-MCA on Ang1-mediated HUVEC junction and tube formation. (A) Effect of 2-MCA on Ang1-mediated Tie2 downstream signals, Akt and p42/44 in HUVECs. HUVECs were cultured with or without Ang1 (500 ng/ml) in the presence of titrated doses of 2-MCA as indicated for 15 min. (B) Effect of 2-MCA on Ang1-mediated membrane stability of the tight junction protein ZO-1. HUVECs were cultured with VEGF (10 ng/ml) with or without Ang1 (100 ng/ml) in the presence or absence of 2-MCA (60 μM) for 24 h, after which ZO-1 expression was assessed immunocytochemically. The bar indicates 20 μm. (C) Tube formation analysis. HUVECs were cultured on Matrigels with or without of Ang1 (500 ng/ml) in the presence or absence of titrated doses of 2-MCA as indicated. Bar indicates 250 μm. (D) HUVECs were cultured in the presence or absence of 2-MCA (30 μM) for 24 h and cell death and apoptosis was then evaluated by the expression of Annexin V and PI staining by FACS (upper). Numbers in each quadrant indicate the percentage of cells among total cells. Quantitative evaluation of $PI^-AnnexinV^+$ apoptotic cells and PI^+ dead cells (lower two graphs) ($n = 3$). (E) Effect of 2-MCA on VEGF- or HGF-mediated p42/44 activation in HUVECs. HUVECs were cultured for 15 min. with or without VEGF (100 ng/ml) or HGF (50 ng/ml) in the presence of titrated doses of 2-MCA as indicated.

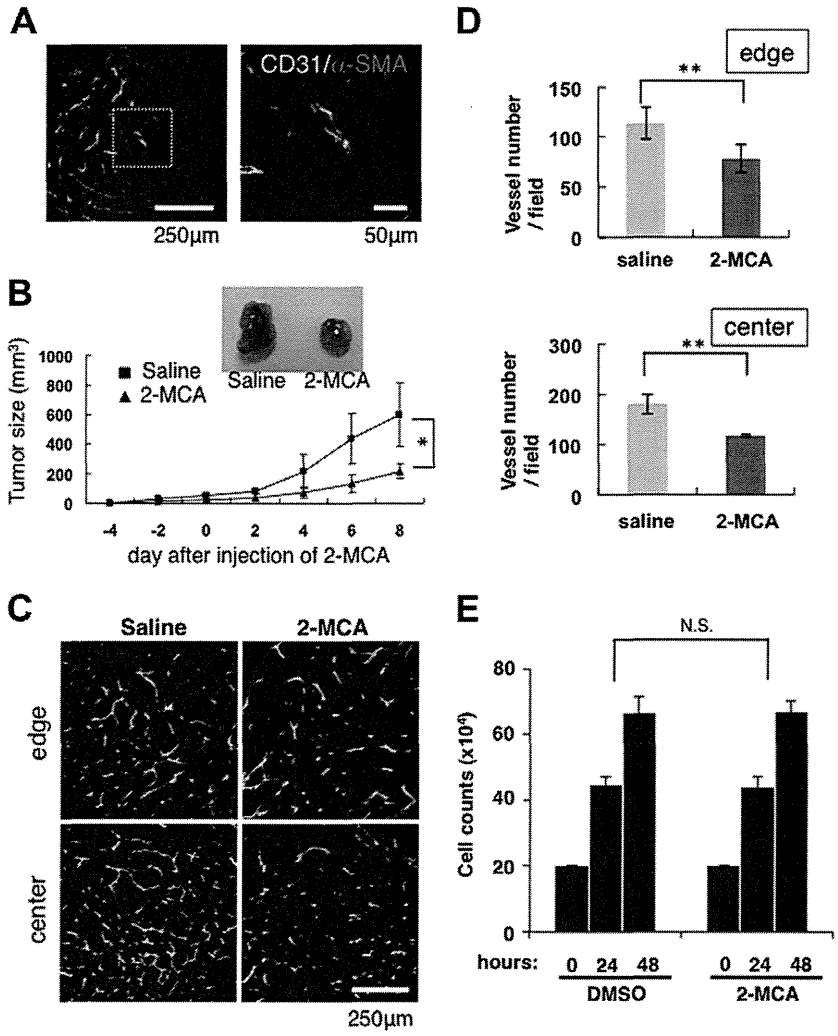

Fig. 3. Effect of 2-MCA on tumor angiogenesis. (A) Blood vessel formation observed in tumors established by inoculating colon26 mouse colon cancer cells. Section of tumor was stained with anti-CD31 (green) and anti-α-SMA (red) antibodies. Right panel shows higher magnification of area indicated by dashed box in the left panel. Bars indicate 250 μm (left) and 50 μm (right). (B) Effect of 2-MCA on tumor growth. 2-MCA (0.5 mg/kg) was injected intraperitoneally every day from day 0 to day 7, starting 4 days after inoculation of tumor cells. Tumor growth was monitored by measuring tumor size. Inset shows gross appearance of tumors dissected on day 8. $^{*}P < 0.05$ ($n = 3$). (C) Suppression of the formation of tumor vasculature by injecting 2-MCA. Sections from the edge and center lesions of the tumor were stained with anti-CD31 antibody. Bar indicates 250 μm. (D) Quantitative evaluation of vascular density calculated for the edge (upper) and center (bottom) of the tumor. The number of blood vessels in 5 random fields was counted. $^{**}P < 0.01$. (E) In vitro proliferation assay using colon26 cells with DMSO or 30 μM 2-MCA.

To investigate direct effects of 2-MCA on ECs, HUVECs were cultured in its presence or absence. Results suggested that the effects of 2-MCA did not depend on enhancement of HUVEC death or apoptosis (Fig. 2D). To further investigate whether the inhibitory effects of 2-MCA were mediated specifically via the angiopoietin/Tie2 pathway, cellular assays were performed to monitor Erk activation by two other angiogenesis-related receptor tyrosine kinases, VEGFR and c-Met, induced by their cognate ligands, VEGF and HGF, respectively. Similar to the results from stimulation by Ang1, both VEGF and HGF were capable of inducing the phosphorylation of Erk. However, no inhibitory effects of 2-MCA were observed on Erk activation by these factors (Fig. 2E). These results indicate that the observed effect of 2-MCA was most likely mediated through specific inhibition of the Ang1-triggered Tie2 activation pathway.

3.3. 2-MCA suppresses tumor growth via inhibition of angiogenesis

Using tumor xenograft models, we previously reported that there are two types of tumor associations with mural cell coverage of ECs in the tumor vasculature [14]. In one type, most blood vessels are not covered with mural cells and greater numbers of vessels develop in the tumor microenvironment. In the other type, mature blood vessels in which ECs are covered with mural cells are observed especially at the edge of the tumor, and the number of vessels is low relative to the first type. We have now tested the effect of 2-MCA on tumor angiogenesis in the first type using the mouse colon cancer cell line, colon26. As shown in Fig. 3A, blood vessels covered with mural cells are rare and angiogenesis is robustly induced in this tumor. Four days after cell inoculation into mice, we started to inject 2-MCA daily for 8 days and monitored tumor growth by evaluating tumor volume. The results documented a clear tumor growth inhibitory action of 2-MCA (Fig. 3B). Blood vessel formation was evaluated by dividing the area into edge and center of tumor; vascular density was found to be decreased in both areas (Fig. 3C and D). 2-MCA did not show any suppressive effects on proliferation of colon26 cells themselves in vitro (Fig. 3E). These data suggest that 2-MCA inhibited tumor growth by suppressing tumor angiogenesis.

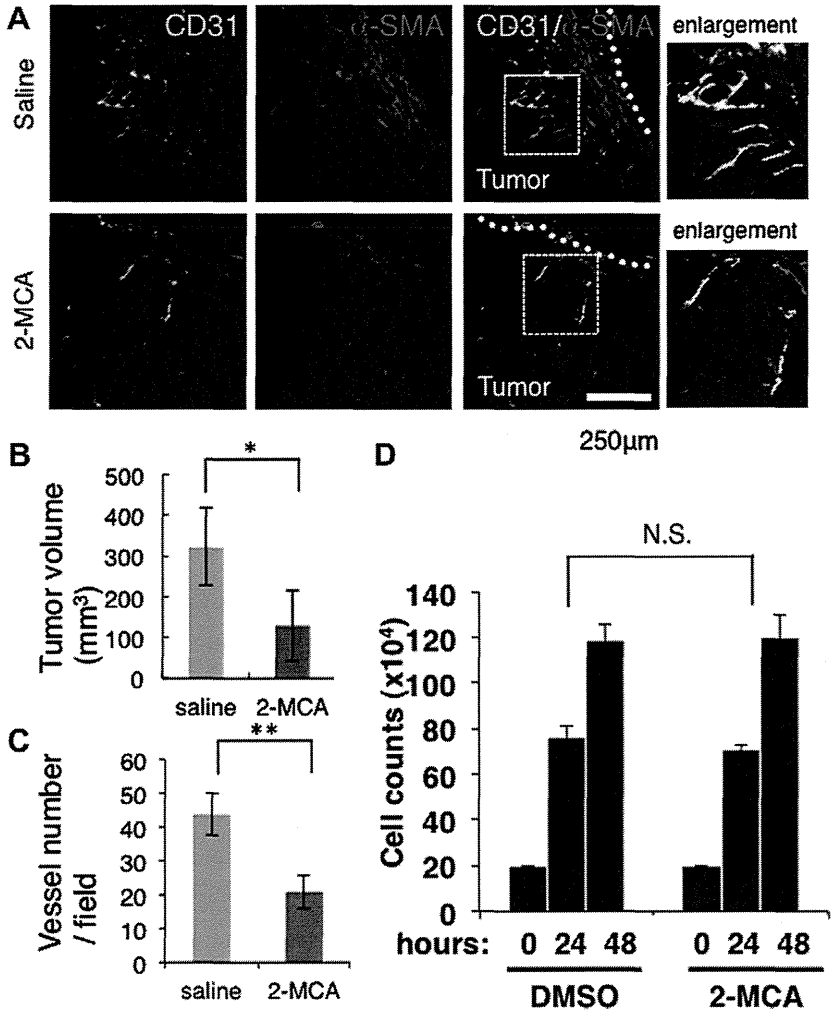

Fig. 4. Effect of 2-MCA on tumor angiogenesis. (A) Blood vessel formation observed in tumors established by inoculation of HCT116 human colon cancer cells. Schedule and doses of 2-MCA were the same as in Fig. 3. Tumors were dissected on day 8 (12 days after tumor cell inoculation) and sections were stained with anti-CD31 (green) and anti-α-SMA (red) antibodies. Right panels show higher magnification of area indicated by dashed box in the left-hand side. Bars indicate 250 μm. (B) Effect of 2-MCA on tumor growth. $^{*}P < 0.05$ ($n = 3$). (C) Quantitative evaluation of vascular density. The number of blood vessels in 5 random fields was counted. $^{**}P < 0.01$. (D) In vitro proliferation assay using HCT116 cells with DMSO or 30 μM 2-MCA.

3.4. 2-MCA inhibits maturation of the tumor vasculature

Using the human colon cancer cell line HCT116 in a xenograft model, we observed very few blood vessels in the center of the tumor but mature vessels covered with mural cells were plentiful at the periphery (Fig. 4A). To investigate whether 2-MCA affects maturation of blood vessels in the tumor environment, we injected it using the same schedule as described in Fig. 3B. Twelve days inoculation of tumor cells, the tumor volume was significantly smaller in the 2-MCA-injected group than in controls (Fig. 4B). Moreover, vascular density was also significantly reduced in the 2-MCA-injected group (Fig. 4A and C). The number of mature blood vessels that were still present in 2-MCA-treated tumors was reduced. 2-MCA did not mediate any direct suppressive effects on HCT116 cell proliferation in vitro (Fig. 4D). These data suggest that 2-MCA affects the maturation of blood vessels by inhibiting mural cell attachment.

4. Discussion

In this work, we screened natural products for Tie2 inhibitory activity and isolated 2-MCA, a small molecule which inhibited tumor growth by suppressing tumor angiogenesis. We cannot completely exclude the possibility that 2-MCA also affected angiogenesis by mechanisms other than Tie2 inhibition, but the finding that 2-MCA blocked Ang1-mediated tube formation and barrier formation implies that its inhibitory action on Tie2 must be at least partly responsible for its suppression of tumor angiogenesis.

One of the objectives of the present study was to identify inhibitors that can block maturation of blood vessels as well as progression of sprouting angiogenesis. This aim arose from the evidence that tumor repopulation is observed from the edge of the tumor even under circumstances where tumor growth seemed to be completely inhibited by treatment with vascular disrupting agents [18]. Similar evidence was also reported that invasion of cancer cells is induced from the edge of the tumor after treatment with angiogenesis inhibitors [19]. We previously reported that blood vessels are fully mature at the edge of the tumor, unlike in its center [14]. Therefore, invasion of cancer cells and repopulation of the tumor after treatment with angiogenesis inhibitors seems to be caused by the resistance of mature blood vessels in the tumor rim to the action of anti-angiogenic drugs. In our present studies using HT116 cells, the number of mature blood vessels in which ECs were covered with mural cells at the edge of the tumor was

reduced by 2-MCA treatment. Therefore, this agent is useful for inhibiting maturation processes of the tumor vasculature during tumor growth.

Constitutively active mutant Tie2 is seen in patients with hereditary venous malformation [15]. Recently, it has been reported that Tie2 constitutively active due to somatic mutation is also found in sporadic venous malformation [20]. Histopathological examination revealed that blood vessels are dilated in a disorderly manner and mural cell attachment is essentially absent in vascular lesions of such patients. Akt activation via Tie2 activation induces maturation of blood vessels. On the other hand, Erk activation via Tie2 activation induces angiogenesis. In the patients with constitutively active Tie2, it is likely that the Erk pathway is strongly activated. As reported here, 2-MCA could inhibit both Erk as well as Akt activation through Tie2 phosphorylation. Therefore, agents like 2-MCA should also be effective for treating lesions in venous malformation as well as tumor angiogenesis.

In terms of Tie2 inhibition, several lines of evidence from studies using soluble Tie2 receptors or aptamers have already suggested that Tie2 inhibition could be effective for suppressing tumor growth [21–23]. However, there is little data on using small molecule Tie2 inhibitors to prevent tumor growth. Although many kinase inhibitors for the VEGF receptor pathway have been developed, Tie2 inhibitors still require more developmental work for expansion of their application to different therapeutic approaches.

Acknowledgments

We thank N. Fujimoto, C. Takeshita for technical assistance. This work was partly supported by the Japanese Ministry of Education, Culture, Sports, Science and Technology, and the Japan Society for Promotion of Science.

References

[1] S.P. Ivy, J.Y. Wick, B.M. Kaufman, An overview of small-molecule inhibitors of VEGFR signaling, Nat. Rev. Clin. Oncol. 6 (2009) 569–579.
[2] H. Hurwitz, L. Fehrenbacher, W. Novotny, et al., Bevacizumab plus irinotecan, fluorouracil, and leucovorin for metastatic colorectal cancer, N. Engl. J. Med. 350 (2004) 2335–2342.
[3] N. Ferrara, H.P. Gerber, J. LeCouter, The biology of VEGF and its receptors, Nat. Med. 9 (2003) 669–676.
[4] H.G. Augustin, G.Y. Koh, G. Thurston, K. Alitalo, Control of vascular morphogenesis and homeostasis through the angiopoietin-Tie system, Nat. Rev. Mol. Cell Biol. 10 (2009) 165–177.
[5] S. Fukuhara, K. Sako, T. Minami, K. Noda, H.Z. Kim, T. Kodama, M. Shibuya, N. Takakura, G.Y. Koh, N. Mochizuki, Differential function of Tie2 at cell-cell contacts and cell-substratum contacts regulated by angiopoietin-1, Nat. Cell Biol. 10 (2008) 513–526.
[6] R.K. Jain, Molecular regulation of vessel maturation, Nat. Med. 9 (2003) 685–693.
[7] D.J. Dumont, G. Gradwohl, G.H. Fong, M.C. Puri, M. Gerstenstein, A. Auerbach, M.L. Breitman, Dominant-negative and targeted null mutations in the endothelial receptor tyrosine kinase, tek, reveal a critical role in vasculogenesis of the embryo, Genes Dev. 8 (1994) 1897–1909.
[8] S. Morozumi, Isolation purification and antibiotic activity of *o*-methoxycinnamaldehyde from *Cinnamon*, Appl. Environ. Microbiol. 36 (1978) 577–583.
[9] H.B. Singh, M. Srivastava, A.B. Singh, A.K. Srivastava, Cinnamon bark oil a potent fungitoxicant against fungi causing respiratory tract mycoses, Allergy 50 (1995) 995–999.
[10] S.T. Chang, P.F. Chen, S.C. Chang, Antibacterial activity of leaf essential oils and their constituents from *Cinnamomum osmophloeum*, J. Ethnopharmacol. 77 (2001) 123–127.
[11] N. Takakura, T. Watanabe, S. Suenobu, Y. Yamada, T. Noda, Y. Ito, M. Satake, T. Suda, A role for hematopoietic stem cells in promoting angiogenesis, Cell 102 (2000) 199–209.
[12] S. Morita, T. Kojima, T. Kitamura, Plat-E: an efficient and stable system for transient packaging of retroviruses, Gene Ther. 7 (2000) 1063–1066.
[13] T. Saitoh, H. Nakano, N. Yamamoto, S. Yamaoka, Lymphotoxin-L receptor mediates NEMO-independent NF-UB activation, FEBS Lett. 532 (2002) 45–51.
[14] N. Satoh, Y. Yamada, Y. Kinugasa, N. Takakura, Angiopoietin-1 alters tumor growth by stabilizing blood vessels or by promoting angiogenesis, Cancer Sci. 99 (2008) 2373–2379.
[15] M. Vikkula, L.M. Boon, K.L. Carraway, J.T. Calvert, A.J. Diamonti, B. Goumnerov, K.A. Pasyk, D.A. Marchuk, M.L. Warman, L.C. Cantley, J.B. Mulliken, B.R. Olsen, Vascular dysmorphogenesis caused by an activating mutation in the receptor tyrosine kinase TIE2, Cell 87 (1996) 1181–1190.
[16] S.W. Lee, W.J. Kim, Y.K. Choi, H.S. Song, M.J. Son, I.H. Gelman, Y.J. Kim, K.W. Kim, SSeCKS regulates angiogenesis and tight junction formation in blood-brain barrier, Nat. Med. 9 (2003) 900–906.
[17] I. Kim, H.G. Kim, S.O. Moon, S.W. Chae, J.N. So, K.N. Koh, B.C. Ahn, G.Y. Koh, Angiopoietin-1 induces endothelial cell sprouting through the activation of focal adhesion kinase and plasmin secretion, Cir. Res. 86 (2000) 952–959.
[18] G.M. Tozer, C. Kanthou, B.C. Baguley, Disrupting tumour blood vessels, Nat. Rev. Cancer 5 (2005) 423–435.
[19] M.P. Ribes, E. Allen, J. Hudock, T. Takeda, H. Okuyama, F. Vinals, M. Inoue, G. Bergers, D. Hanahan, O. Casanovas, Antiangiogenic therapy elicits malignant progression of tumors to increased local invasion and distant metastasis, Cancer Cell 15 (2009) 220–231.
[20] N. Limaye, V. Wouters, M. Uebelhoer, M. Tuominen, R. Wirkkala, J.B. Mulliken, L. Eklund, L.M. Boon, M. Vikkula, Somatic mutations in angiopoietin receptor gene TEK cause solitary and multiple sporadic venous malformations, Nat. Genet. 41 (2009) 118–124.
[21] P. Lin, P. Polverini, M. Dewhirst, S. Shan, P.S. Rao, K. Peters, Inhibition of tumor angiogenesis using a soluble receptor establishes a role for Tie2 in pathologic vascular growth, J. Clin. Invest. 100 (1997) 2072–2078.
[22] R. Tournaire, M.P. Simon, F.I. Noble, A. Eichmann, P. England, J. Pouyssegur, A short synthetic peptide inhibits signal transduction, migration and angiogenesis mediated by Tie2 receptor, EMBO Rep. 5 (2004) 262–267.
[23] Y.J. Koh, H.Z. Kim, S.I. Hwang, J.E. Lee, N. Oh, K. Jung, M. Kim, K.E. Kim, H. Kim, N.K. Lim, C.J. Jeon, G.M. Lee, B.H. Jeon, D.H. Nam, H.K. Sung, A. Nagy, O.J. Yoo, G.Y. Koh, Double antiangiogenic protein, DAAP, targeting VEGF-A and angiopoietins in tumor angiogenesis, metastasis, and vascular leakage, Cancer Cell 18 (2010) 171–184.

UICC
global cancer control

IJC
International Journal of Cancer

Reaction of plasma hepatocyte growth factor levels in non-small cell lung cancer patients treated with EGFR-TKIs

Hidenori Tanaka[1], Tatsuo Kimura[1], Shinzoh Kudoh[1], Shigeki Mitsuoka[1], Tetsuya Watanabe[1], Tomohiro Suzumura[1], Keisei Tachibana[2], Masayuki Noguchi[2], Seiji Yano[3] and Kazuto Hirata[1]

[1] Department of Respiratory Medicine, Graduate School of Medicine, Osaka City University, Abeno-ku, Osaka, Japan
[2] Department of Pathology, Institute of Basic Medical Science, Graduate School of Comprehensive Human Sciences, University of Tsukuba, Tsukuba, Japan
[3] Division of Medical Oncology, Cancer Research Institute, Kanazawa University, Kanazawa, Japan

Hepatocyte growth factor induces resistance to epidermal growth factor receptor tyrosine kinase inhibitors. It has been hypothesized that epidermal growth factor receptor tyrosine kinase inhibitors administration may influence the levels of plasma hepatocyte growth factor. Patients with advanced non-small cell lung cancer and relapsed after chemotherapies were eligible. Plasma hepatocyte growth factor levels were analyzed on pretreatment and post-treatment day 15 and 30. We also investigated the correlation between plasma hepatocyte growth factor levels and sensitivity to epidermal growth factor receptor tyrosine kinase inhibitors, tissue immunoreactivity for hepatocyte growth factor and *MET* gene status. Thirty-one patients were enrolled. Plasma hepatocyte growth factor levels on post-treatment day 15 (630.1 ± 366.9 pg/ml) were significantly higher ($p = 0.029$) than the pretreatment plasma hepatocyte growth factor levels (485.9 ± 230.2 pg/ml). Plasma hepatocyte growth factor levels on the post-treatment day 30 (581.5 ± 298.1 pg/ml) tend to be higher than those before treatment ($p = 0.057$). Pretreatment plasma hepatocyte growth factor levels in patients with progressive disease (724.1 ± 216.4 pg/ml) were significantly higher than those in patients with stable disease (396.5 ± 148.3 pg/ml; $p = 0.0008$) and partial response (381.7 ± 179.0 pg/ml; $p = 0.0039$). The optimal pretreatment plasma hepatocyte growth factor cut-off value for diagnosis of responder was 553.5 pg/ml, and its sensitivity and specificity were 90% and 65%, respectively. Pretreatment plasma hepatocyte growth factor levels had no correlation with tissue immunoreactivities for hepatocyte growth factor, *MET* gene status and active *EGFR* mutations. Administration of epidermal growth factor receptor tyrosine kinase inhibitors significantly increased plasma hepatocyte growth factor levels. High levels of pretreatment plasma hepatocyte growth factor indicated intrinsic resistance to epidermal growth factor receptor tyrosine kinase inhibitors. Plasma hepatocyte growth factor can serve as a useful biomarker for the early diagnosis of tumor relapse treated with epidermal growth factor receptor tyrosine kinase inhibitors.

Key words: EGFR-TKIs, hepatocyte growth factor, non-small cell lung cancer, EGFR mutation, MET

Abbreviations: DAB: 3,3′-diaminobenzidine tetrahydrochloride; DAPI: 4,6-diamidino-2-phenylindole; EGFR-TKIs: epidermal growth factor receptor-tyrosine kinase inhibitors; FISH: fluorescence in situ hybridization; FITC: fluorescein isothiocyanate; HGF: Hepatocyte growth factor; NSCLC: non-small cell lung cancer; PBS: phosphate buffered saline; PD: progressive disease; PI3K: phosphatidylinositol-3-kinase; PNA-LNA PCR: peptide nucleic acid-locked nucleic acid polymerase chain reaction; PR: partial response; ROC: receiver-operating characteristic; SD: stable disease; SD: standard deviation

Grant sponsor: Chugai Pharmaceutical
DOI: 10.1002/ijc.25799
History: Received 11 Aug 2010; Accepted 20 Oct 2010; Online 2 Dec 2010

Correspondence to: Hidenori Tanaka, M.D., Department of Respiratory Medicine, Graduate School of Medicine, Osaka City University, 1-4-3 Asahi-machi, Abeno-ku, Osaka 545-8585, Japan, Tel.: 81-6-6645-3801, Fax: +81-6-6646-6808, E-mail: hidetanaka@nike.eonet.ne.jp

Lung cancer is the leading cause of cancer-related death worldwide, largely because most patients are diagnosed at advanced stages.[1,2] Recent strategies for treating non-small cell lung cancer (NSCLC) have focused on the development of molecular-targeted therapies, such as those including epidermal growth factor receptor-tyrosine kinase inhibitors (EGFR-TKIs) of erlotinib and gefitinib. The tumors with active *EGFR* mutations are extremely sensitive to EGFR-TKIs. However, disease progression usually occurs in most patients at 6–12 months after EGFR-TKI treatments. Acquired EGFR-TKIs resistance has been associated with the development of a secondary mutation of T790M in *EGFR*.[3,4] In addition, *MET* amplification has been identified as another mechanism of acquired resistance.[5,6]

Recently, Yano *et al.* reported that hepatocyte growth factor (HGF) induces EGFR-TKIs resistance by restoring the phosphatidylinositol-3-kinase (PI3K)/AKT signaling pathway *via* phosphorylation of MET.[7] HGF was first identified in the serum of hepatectomized rats as a potent growth factor of hepatocytes.[8] HGF is secreted in response to injury by many

organs such as the mammary gland, kidneys, liver and lungs.[9,10] HGF is produced by various cells, especially tumor cells, fibroblast cells and endothelial cells.[11,12] HGF induces multiple biological effects in target cells, including proliferation and survival, angiogenesis, cell migration and invasion and morphogenesis and tissue organization.[13,14] Tumor tissue specimens that stain strongly for HGF indicate poor outcome after NSCLC resection.[15] However, the mechanism regulating plasma HGF level in NSCLC patients has been investigated to a limited extent. It has been hypothesized that EGFR-TKIs administration may influence the levels of plasma HGF. In this study, we evaluated the pretreatment and post-treatment plasma HGF levels after EGFR-TKIs administration in advanced NSCLC. We also investigated the correlation between plasma HGF levels and sensitivity to EGFR-TKIs, tissue immunoreactivity for HGF and *MET* gene status. In addition, we determined a cut-off value of pretreatment plasma HGF level to discriminate sensitive from resistant populations, and evaluated the association between the resultant cut-off value and presence of active *EGFR* mutations.

Material and Methods

Patients

Patients with histologically or cytologically confirmed advanced NSCLC and relapsed after one or two prior chemotherapies were eligible. Each patient was required to meet the following criteria: adequate organ functions, performance status of 0-2, and no other active malignancies. Mutations in the tyrosine kinase domain (exons 18–21) of *EGFR* were identified by peptide nucleic acid-locked nucleic acid polymerase chain reaction (PNA-LNA PCR) clamp assay. Written informed consent was obtained from all patients. This study was approved by the Osaka City University Hospital Institutional Review Boards.

Treatment, response and clinical outcome

EGFR-TKIs (erlotinib 150 mg/day, gefitinib 250 mg/day) were administered once daily. The treatment was continued until the disease progression or the patient developed intolerable toxicity or withdrew his/her consent to continue participation in the study. The objective tumor responses of each examined lesion were assessed every 4 weeks after EGFR-TKIs administration according to the Response Evaluation Criteria in Solid Tumors, ver1.0. Toxicity was graded according to the National Cancer Institute Common Toxicity Criteria Version 3.0 criteria. The grade 3 and 4 of EGFR-TKIs-related nonhematologic toxicities were managed by reducing the dose of EGFR-TKIs.

Plasma HGF analysis

Plasma samples were collected pretreatment and on post-treatment days 15 and day 30. Venous blood (7 ml) was collected in EDTA (anticoagulant)-containing tubes and immediately centrifuged at 3,000 rpm for 15 minutes. Plasma samples were frozen at −80°C until analysis. Plasma HGF levels were analyzed by Luminex 200 PONENT system (Milliplex MAP kits; Millipore) according to the manufacturer's instructions. Plasma HGF levels were estimated as previously reported;[16] in brief, 25 μl of plasma was incubated with antibody-linked beads overnight at 4°C, washed twice with the washing solution, and incubated for 1 hour with biotinylated secondary antibodies. Data acquisition using the Luminex system was performed after a final incubation of 30 minutes with streptavidin-phycoerythrin. The minimum detectable concentration of HGF was 19.2 pg/ml. All the samples were assayed in duplicate.

Immunohistochemical staining of HGF

Immunohistochemical staining of HGF was performed as previously reported.[17] Briefly, we used a 1:20 dilution of a rabbit polyclonal antibody against HGF-α (IBL, Gunma, Japan). Immunohistochemical staining was performed using formalin-fixed paraffin-embedded tissue sections obtained from our NSCLC patients. Endogenous peroxidase was blocked with 3% aqueous H_2O_2 solution for 30 minutes, and the sections (4-μm thick) were deparaffinized in xylene and rehydrated in decreasing concentrations of ethanol. Microwave antigen retrieval was performed in 0.01 M citrate buffer (pH 6.0). The sections were treated with primary antibodies for 1 hour at room temperature, washed with phosphate buffered saline (PBS) and treated with EnVision/HRP polymer reagent (Dako, Glostrup, Denmark) for 30 minutes at room temperature. The immunostained sections were treated with 3,3′-diaminobenzidine tetrahydrochloride (DAB) solution (Dako, Glostrup, Denmark). Omission of primary antibodies served as negative controls. The immunoreactivities of the samples were independently evaluated by 2 investigators (KT and MN).

The scoring index was obtained as the product of percentage and intensity of the immunostained sections in the range 0–300, according to the method of Turke *et al.* with slight modifications.[18,19] In brief, the tissue immunoreactivity for HGF was evaluated as the percentage of cancer cells with positive cytoplasmic and/or membranous staining (0–100%), and the model intensity of the positively stained cells was determined on a scale of 0 to 3+ (0, complete absence of staining; 1+, staining weaker than that of the normal bronchial epithelium; 2+, staining similar to the that of the normal bronchial epithelium; 3+, staining clearly more intense than that of the normal bronchial epithelium).

Fluorescence in situ hybridization analyses of MET

MET fluorescence *in situ* hybridization (FISH) analyses were performed as previously reported.[19] Briefly, 4-μm thick serial sections from each tissue block were analyzed by a dual-color FISH by using a MET/CEP7 probe cocktail (Kreatech Diagnostics, Amsterdam, The Netherlands). After deparaffinization and dehydration, the slides were immersed in 0.2N HCl, incubated in 1 M NaSCN for 30 minutes at 80°C, and immersed in a pepsin solution for 15–45 minutes at 37°C.

The DNA probe set was applied onto the slides; subsequently, the slides were incubated on a hot plate at 80°C for 5 minutes to allow attachment of the target DNA and the probe, and incubated again at 37°C for 16 hours to achieve hybridization. Then, posthybridization washes were performed using 0.4× SSC/0.3% NP-40 for 2 minutes at 72°C and subsequently with 2×SSC/0.1% NP-40 for 1 minute at room temperature. The slides were counterstained with 4,6-diamidino-2-phenylindole (DAPI) and an antifade compound (*p*-phenylenediamine). The FISH signals were enumerated in at least 100 nonoverlapping tumor cell nuclei by using an epifluorescence microscope with single interference filters sets for green (fluorescein isothiocyanate, FITC), red (Texas red) and blue (DAPI), and using dual (red/green) and triple (blue, red and green) band pass filters. According to the copy number of the *MET* gene, the following 6 categories were established: disomy (≤2 copies in >90% of cells); low trisomy (≤2 copies in ≥40% of cells, 3 copies in 10–40% of cells and ≥4 copies in <10% of cells); high trisomy (≤2 copies in ≥40% of cells, 3 copies in ≥40% of cells and ≥4 copies in <10% of cells); low polysomy (≥4 copies in 10–40% of cells); high polysomy (≥4 copies in ≥40% of cells); and gene amplification (presence of tight *MET* gene clusters and *MET* gene to chromosome 7 ratio of ≥2 or ≥15 copies of Met per cell in ≥10% of cells).[20,21] The *MET* gene status was further classified into three groups: *MET* FISH-negative (disomy, low trisomy, high trisomy and low polysomy), *MET* FISH-positive with high polysomy, and *MET* FISH-positive with gene amplification.

Statistical analysis

Statistical analyses were performed by using the Student's *t*-test (Stat View5.0 and JMP8.0 statistical program). All values are expressed as mean and standard deviation (SD). The association between pretreatment plasma HGF concentrations and responses to EGFR-TKIs was compared by Kruskal-Wallis test. The best cut-off value for diagnosis of responder (PR plus SD patients) was investigated by receiver-operating characteristic (ROC) analysis, and its sensitivity and specificity were calculated. The association between the resultant cut-off value and presence of active *EGFR* mutations was performed with Fisher's exact test. The relation between plasma HGF concentrations and scoring indexes of both HGF immunoreactivity and *MET* gene status was investigated by Pearson's correlation coefficient test. A p value of less than 0.05 was considered statistically significant.

Results

Patient characteristics

Between September 2008 and October 2009, 31 patients were enrolled in this study. We could not obtain adequate plasma samples for analyses from 3 patients on pretreatment, 6 patients on the post-treatment day 15, and 8 patients on the post-treatment day 30. *EGFR* mutation status was positive in 19 patients, negative in 9 patients, and unknown in 3 patients. Initially, no patients with *EGFR* mutations had the secondary T790M mutation. The patient population profile is provided in Tables 1 and 2.

Table 1. Patient characteristics (n = 31)

Characteristic	Number of patients
Age	
Median (range)	67 (54–86)
Gender	
Male/female	17/14
Performance status	
0/1/2	3/22/6
Clinical stage	
IIIB/IV	6/25
Histology	
Adenocarcinoma	28
Squamous	2
Large cell	1
Smoking history	
Never	11
Former	20

Plasma HGF levels before and after EGFR-TKIs treatment

Plasma HGF levels were analyzed in 28 of the 31 patients before treatment, in 25 patients on the post-treatment day 15, and in 23 patients on the post-treatment day 30. The mean pretreatment plasma HGF level was 485.9 ± 230.2 pg/ml. The association between plasma HGF levels and EGFR-TKIs treatment is shown in Figure 1. Plasma HGF levels on the post-treatment day 15 (630.1 ± 366.9 pg/ml) were significantly increased as compared to the pretreatment plasma HGF levels (p = 0.029). Plasma HGF levels on the post-treatment day 30 (581.5 ± 298.1 pg/ml) tend to be higher than those before treatment (p = 0.057).

Association between pretreatment plasma HGF levels and the efficacy of EGFR-TKIs treatment

We analyzed the association between pretreatment plasma HGF levels and the efficacy of EGFR-TKIs treatment in 28 patients (Fig. 2). The response to EGFR-TKIs treatment was partial response (PR) in 8 cases, stable disease (SD) in 12 cases and progressive disease (PD) in 8 cases. The 8 PR cases, 8 of 12 SD cases and 3 of 8 PD cases had *EGFR* mutations. Pretreatment plasma HGF levels in PD patients (724.1 ± 216.4 pg/ml) were significantly higher as compared to those in SD patients (396.5 ± 148.3 pg/ml; p = 0.0008) and PR patients (381.7 ± 179.0 pg/ml; p = 0.0039).

In the ROC analysis, the optimal pretreatment plasma HGF cut-off value for diagnosis of responder (PR plus SD patients) was 553.5 pg/ml. In Figure 2, the horizontal dash

Table 2. Summary of pretreatment plasma HGF and tissue samples from patients with NSCLC

Case	Response to EGFR-TKIs	Pretreatment plasma HGF (pg/ml)	*EGFR* mutation	HGF IHC	*MET*
1	PR	112.3	Ex21 (L858R)	Low	Positive
2	PR	245.0	Ex19 (E746-A750Del)	Strong	Negative
3	PR	257.6	Ex21 (L858R)	Low	Negative
4	PR	303.3	Ex21 (L858R)	High	Positive
5	PR	449.6	Ex19 (E746-A750Del)	High	Amplification
6	PR	508.5	Ex21(L858R) +Ex19(E746-A750Del)	Low	Negative
7	PR	538.0	E746-A750Del	Low	Negative
8	PR	639.5	Ex21 (L858R)	Low	Negative
9	SD	185.8	Ex19 (E476-A750Del)	N.E	N.E
10	SD	188.1	Ex21 (L858R)	Low	Negative
11	SD	208.0	Negative	Low	Negative
12	SD	331.3	Ex21 (L858R) + Ex19 (E747-S752Del)	Low	Negative
13	SD	335.4	Ex19 (E746-A750Del)	Strong	Negative
14	SD	421.0	Ex21 (L858R)	High	Negative
15	SD	432.1	Ex19 (E746-A750Del)	Low	Negative
16	SD	481.1	Negative	Low	Negative
17	SD	487.8	Ex19	High	Positive
18	SD	494.6	Negative	N.E	N.E
19	SD	553.5	Ex19	Low	Negative
20	SD	639.5	Negative	N.E	N.E
21	SD	N.E	Unknown	N.E	N.E
22	SD	N.E	Unknown	N.E	N.E
23	PD	432.1	Negative	Strong	Positive
24	PD	481.1	Negative	Low	Positive
25	PD	639.5	Ex19	High	Negative
26	PD	678.0	Ex21 (L858R)	Low	Positive
27	PD	688.0	Negative	High	Positive
28	PD	882.0	Negative	Low	Unknown
29	PD	989.1	Negative	Low	Negative
30	PD	1003.1	Ex18	High	Positive
31	PD	N.E	Unknown	N.E	N.E

Abbreviations: N.E: not evaluated; PD: progressive disease; SD: stable disease; PR: partial response; L858R: L858R point mutation; Del: in-frame deletion.

line showed the cut-off value of 553.5 pg/ml. Its sensitivity and specificity were 90% and 65%, respectively. The area under the curve for pretreatment plasma HGF levels was 0.888. Furthermore, we investigated whether this cut-off value is associated with presence of active *EGFR* mutations. However, pretreatment plasma HGF cut-off value had no correlation with presence of active *EGFR* mutation (p=0.405).

The most frequent adverse events were rash and diarrhea. Grade 2 rash and diarrhea occurred in 9 (29%) and 4 (13%) patients, respectively. Grade 3 diarrhea occurred in 1 (3%) patient. Adverse events had no correlation with the pretreatment plasma HGF levels.

Tissue immunoreactivities for HGF and MET gene status

To clarify the source of plasma HGF, we evaluated the tissue immunoreactivity for HGF and the *MET* status by FISH in 25 of the 31 patients. Six patients were diagnosed NSCLC only cytologically. Tumor samples were collected from 25 patients, including surgically resected specimens from 8 patients, transbronchial biopsy specimens from 15 patients

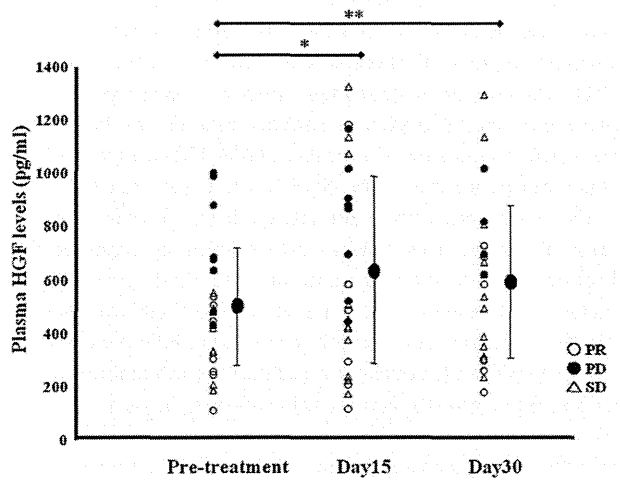

Figure 1. Changes in plasma HGF levels before and after EGFR-TKIs treatment in lung cancer patients. Plasma HGF levels on post-treatment day 15 (630.1 ± 336.9 pg/ml) were significantly increased as compared to the pretreatment HGF levels (485.9 ± 230.2 pg/ml) (*$p = 0.029$). Plasma HGF levels on post-treatment day 30 (581.5 ± 298.1 pg/ml) were higher than those before treatment (**$p = 0.057$).

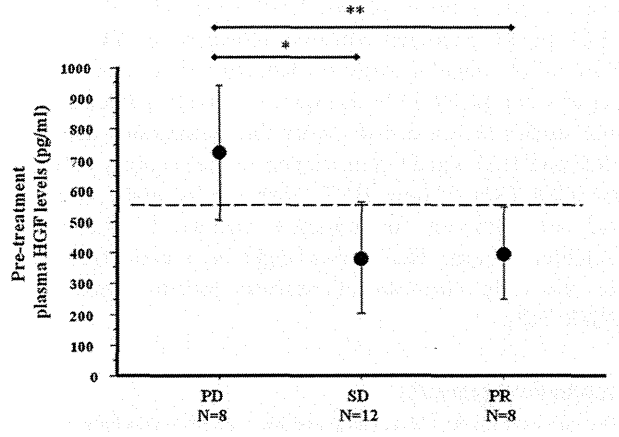

Figure 2. Relationship between pretreatment plasma HGF levels and the efficacy of EGFR-TKIs treatment. Pretreatment plasma HGF levels in PD patients ($n = 8$; 724.1 ± 216.4 pg/ml) were significantly higher as compared to those in PR patients ($n = 8$; 381.7 ± 179.0 pg/ml; **$p = 0.0039$) and SD patients ($n = 12$; 396.5 ± 148.3 pg/ml; *$p = 0.0008$). The horizontal dash line showed the optimal pretreatment plasma HGF cut-off value of 553.5 pg/ml for diagnosis of responders (PR plus SD patients).

and biopsy specimens from vertebra and skin in each 1 patient. High HGF expression (index score over 150) was detected in 10 of the 25 (40%) specimens and strong expression in 3 specimens (12%) with HGF immunoreactivity scoring index of more than 200.

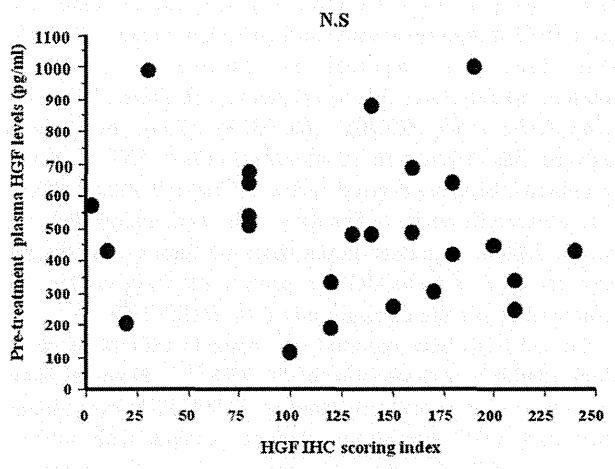

Figure 3. Pretreatment plasma HGF levels had no correlation with the scoring indexes of HGF immunoreactivity ($r = -0.088$, $p = 0.678$).

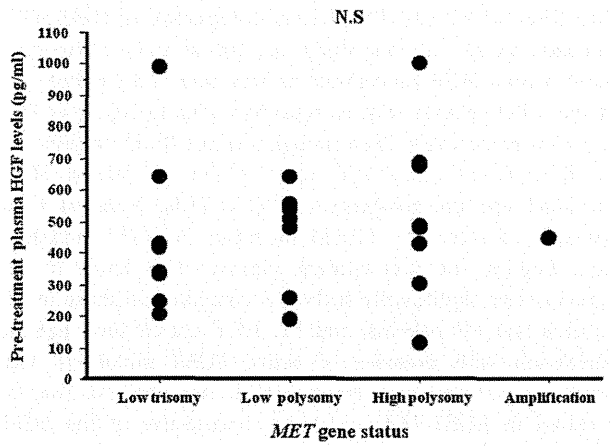

Figure 4. Pretreatment plasma HGF levels had no correlation with MET gene status ($r = 0.176$, $p = 0.414$).

FISH revealed that 9 patients (36%) were *MET* positive (1 with gene amplification and 8 with high polysomy). Pretreatment plasma HGF levels had no correlation with the scoring indexes of both HGF immunoreactivity ($r = -0.088$, $p = 0.678$) and *MET* gene status ($r = 0.176$, $p = 0.414$) (Figs. 3 and 4). Further, response to EGFR-TKIs was not associated with the scoring indexes of HGF immunoreactivity and *MET* gene status.

Discussion

We have shown that plasma HGF levels on the post-treatment day 15 were significantly increased as compared to the pretreatment plasma levels, and the HGF concentration continued to remain high up to day 30. Pretreatment plasma

HGF levels had no correlation with the scoring indexes of both HGF immunoreactivity and *MET* gene status. Recently, Wei Wang *et al.* reported that treatment of the *EGFR* mutant human lung adenocarcinoma cell lines, PC-9 (del E746_A750) and HCC827 (del E746_A750), by gefitinib induced the recruitment of fibroblast cells.[22] HGF is a predominant fibroblast-derived factor.[23] These findings indicate that other cells such as fibroblast cells and endothelial cells secrete HGF to a greater extent than the tumor cells; the former cell types secrete HGF to protect the lung cancer cells from and repair the damage caused by EGFR-TKIs.

Several trials have reported that patients with *EGFR* mutations exhibit a response rate of 70–75%.[24–27] However, some patients are intrinsically resistant to EGFR TKIs even though they have *EGFR* mutations. Among patients with intrinsic resistance, only 0.5 and 3% patients have the secondary T790M mutation and *MET* amplification, respectively.[6,28] HGF have been reported as third mechanism of EGFR-TKIs resistance.[7] Kasahara *et al.* reported that lung adenocarcinoma patients with *EGFR* mutation did not affect serum HGF levels and that the serum HGF levels in PD patients were higher than those in SD and PR patients, irrespective of their *EGFR* mutation status.[29] In our study, the cut-off value of pretreatment plasma HGF concentrations was over 553.5 pg/ml in 6 of the 8 PD patients with its sensitivity and specificity of 90% and 65%, respectively. Even though 3 of the 8 PD patients had *EGFR* mutations and high concentrations of plasma HGF, they had intrinsic resistance to EGFR-TKIs. None of these patients had secondary T790M mutation and *MET* amplification. Besides, the pretreatment plasma HGF levels in PD patients were significantly higher as compared to those in SD patients and PR patients, and the HGF cut-off level had no correlation with presence of active *EGFR* mutations. Our results suggest that high plasma HGF concentrations may be involved in EGFR-TKIs resistance, irrespective of the *EGFR* mutation status.

Further, we investigated the correlation between plasma HGF concentration, tissue immunoreactivity for HGF, *MET* gene status and the efficacy of EGFR-TKIs treatment. The pretreatment plasma HGF levels had no association with tissue immunoreactivity for HGF and *MET* gene status. In addition, response to EGFR-TKIs treatment had no association with tissue immunoreactivity for HGF and *MET* gene status. Cappuzzo *et al.* reported that patients with primary resistance to gefitinib therapy could not be identified by *MET* FISH analysis of pretreatment tumor biopsy specimens.[19] Our results may provide the evidence that plasma HGF levels are a better indicator of intrinsic EGFR-TKIs resistance than tissue immunoreactivity for HGF or *MET* gene status.

Our study has certain limitations. First, plasma HGF has been influenced from various factors such as renal or liver dysfunction, interstitial pneumonia, and other active malignancies. We excluded the patients who had the possible interfering factors in the analysis of plasma HGF levels. However, we could not completely exclude the influencing factors such as other growth factors and cytokines. Second, the number of patients enrolled in this study was small. Third, we collected blood samples at only 3 time points (pretreatment and on post-treatment days 15 and 30). By measuring plasma HGF levels at more time points, we could evaluate the relationship between acquired resistance to EGFR-TKIs and plasma HGF levels. Finally, in the evaluation of the tissue immunoreactivity for HGF, there was some difference in evaluating the percent positivity for HGF between the small biopsy specimen of transbronchial tissue and the large specimen of surgically resected tissue.

In conclusion, statistically significant increase in plasma HGF levels was observed on administering EGFR-TKIs. High levels of pretreatment plasma HGF, which cut-off level was 553.5 pg/ml, indicated intrinsic resistance to EGFR-TKIs. This cut-off value is useful in defining a case as positive or negative for EGFR-TKIs therapy for relevant clinicians. Further studies are needed to clarify the mechanisms of plasma HGF and HGF signaling in relation to the acquired resistance to EGFR-TKIs. Plasma HGF levels can be easily measured and are sufficient for objective analysis of the patient condition. Plasma HGF levels might be a useful biomarker for the early diagnosis of relapsed patients treated with EGFR-TKIs.

Acknowledgements

The authors thank Ms. Maki Nakai and Ms. Mari Okamoto for their secretarial assistance. Dr. S. Yano has received commercial research support from Chugai Pharmaceutical Co., Ltd.

References

1. Parkin D, Bray F, Ferlay J, Pisani P. Global cancer statistics, 2002. *CA Cancer J Clin* 2005;55:74–108.
2. Jemal A, Siegel R, Ward E, Murray T, Xu J, Thun M. Cancer statistics, 2007. *CA Cancer J Clin* 2007;57:43–66.
3. Kobayashi S, Boggon T, Dayaram T, Jänne P, Kocher O, Meyerson M, Johnson B, Eck M, Tenen D, Halmos B. EGFR mutation and resistance of non-small-cell lung cancer to gefitinib. *N Engl J Med* 2005;352:786–92.
4. Pao W, Miller V, Politi K, Riely G, Somwar R, Zakowski M, Kris M, Varmus H. Acquired resistance of lung adenocarcinomas to gefitinib or erlotinib is associated with a second mutation in the EGFR kinase domain. *PLoS Med* 2005;2:e73.
5. Engelman J, Zejnullahu K, Mitsudomi T, Song Y, Hyland C, Park J, Lindeman N, Gale C, Zhao X, Christensen J, Kosaka T, Holmes A, et al. MET amplification leads to gefitinib resistance in lung cancer by activating ERBB3 signaling. *Science* 2007;316:1039–43.
6. Bean J, Brennan C, Shih J, Riely G, Viale A, Wang L, Chitale D, Motoi N, Szoke J, Broderick S, Balak M, Chang W, et al. MET amplification occurs with or without T790M mutations in EGFR mutant lung tumors with acquired resistance to gefitinib or erlotinib. *Proc Natl Acad Sci USA* 2007;104:20932–7.
7. Yano S, Wang W, Li Q, Matsumoto K, Sakurama H, Nakamura T, Ogino H,

Kakiuchi S, Hanibuchi M, Nishioka Y, Uehara H, Mitsudomi T, et al. Hepatocyte growth factor induces gefitinib resistance of lung adenocarcinoma with epidermal growth factor receptor-activating mutations. *Cancer Res* 2008;68:9479–87.
8. Nakamura T, Nawa K, Ichihara A. Partial purification and characterization of hepatocyte growth factor from serum of hepatectomized rats. *Biochem Biophys Res Commun* 1984;122:1450–9.
9. Igawa T, Kanda S, Kanetake H, Saitoh Y, Ichihara A, Tomita Y, Nakamura T. Hepatocyte growth factor is a potent mitogen for cultured rabbit renal tubular epithelial cells. *Biochem Biophys Res Commun* 1991;174:831–8.
10. Yamashita J, Ogawa M, Yamashita S, Nomura K, Kuramoto M, Saishoji T, Shin S. Immunoreactive hepatocyte growth factor is a strong and independent predictor of recurrence and survival in human breast cancer. *Cancer Res* 1994;54: 1630–3.
11. Birchmeier C, Birchmeier W, Gherardi E, Vande Woude G. Met, metastasis, motility and more. *Nat Rev Mol Cell Biol* 2003;4: 915–25.
12. Bhowmick N, Neilson E, Moses H. Stromal fibroblasts in cancer initiation and progression. *Nature* 2004;432:332–7.
13. Jiang W, Hiscox S, Matsumoto K, Nakamura T. Hepatocyte growth factor/ scatter factor, its molecular, cellular and clinical implications in cancer. *Crit Rev Oncol Hematol* 1999;29:209–48.
14. Comoglio P, Boccaccio C. Scatter factors and invasive growth. *Semin Cancer Biol* 2001;11:153–65.
15. Siegfried J, Weissfeld L, Luketich J, Weyant R, Gubish C, Landreneau R. The clinical significance of hepatocyte growth factor for non-small cell lung cancer. *Ann Thorac Surg* 1998;66:1915–8.
16. Leng S, McElhaney J, Walston J, Xie D, Fedarko N, Kuchel G. ELISA and multiplex technologies for cytokine measurement in inflammation and aging research. *J Gerontol A Biol Sci Med Sci* 2008;63:879–84.
17. Suzuki K, Cheng J, Watanabe Y. Hepatocyte growth factor and c-Met (HGF/c-Met) in adenoid cystic carcinoma of the human salivary gland. *J Oral Pathol Med* 2003;32:84–9.
18. Turke A, Zejnullahu K, Wu Y, Song Y, Dias-Santagata D, Lifshits E, Toschi L, Rogers A, Mok T, Sequist L, Lindeman N, Murphy C, et al. Preexistence and clonal selection of MET amplification in EGFR mutant NSCLC. *Cancer Cell* 2010;17:77–88.
19. Cappuzzo F, Jänne P, Skokan M, Finocchiaro G, Rossi E, Ligorio C, Zucali P, Terracciano L, Toschi L, Roncalli M, Destro A, Incarbone M, et al. MET increased gene copy number and primary resistance to gefitinib therapy in non-small-cell lung cancer patients. *Ann Oncol* 2009;20:298–304.
20. Cappuzzo F, Hirsch F, Rossi E, Bartolini S, Ceresoli G, Bemis L, Haney J, Witta S, Danenberg K, Domenichini I, Ludovini V, Magrini E, et al. Epidermal growth factor receptor gene and protein and gefitinib sensitivity in non-small-cell lung cancer. *J Natl Cancer Inst* 2005;97:643–55.
21. Hirsch F, Herbst R, Olsen C, Chansky K, Crowley J, Kelly K, Franklin W, Bunn PJ, Varella-Garcia M, Gandara D. Increased EGFR gene copy number detected by fluorescent in situ hybridization predicts outcome in non-small-cell lung cancer patients treated with cetuximab and chemotherapy. *J Clin Oncol* 2008;26: 3351–7.
22. Wang W, Li Q, Yamada T, Matsumoto K, Matsumoto I, Oda M, Watanabe G, Kayano Y, Nishioka Y, Sone S, Yano S. Crosstalk to stromal fibroblasts induces resistance of lung cancer to epidermal growth factor receptor tyrosine kinase inhibitors. *Clin Cancer Res* 2009;15:6630–8.
23. Nakamura T, Matsumoto K, Kiritoshi A, Tano Y. Induction of hepatocyte growth factor in fibroblasts by tumor-derived factors affects invasive growth of tumor cells: in vitro analysis of tumor-stromal interactions. *Cancer Res* 1997; 57:3305–13.
24. Mok T, Wu Y, Thongprasert S, Yang C, Chu D, Saijo N, Sunpaweravong P, Han B, Margono B, Ichinose Y, Nishiwaki Y, Ohe Y, et al. Gefitinib or carboplatin-paclitaxel in pulmonary adenocarcinoma. *N Engl J Med* 2009;361:947–57.
25. Rosell R, Moran T, Queralt C, Porta R, Cardenal F, Camps C, Majem M, Lopez-Vivanco G, Isla D, Provencio M, Insa A, Massuti B, et al. Screening for epidermal growth factor receptor mutations in lung cancer. *N Engl J Med* 2009;361: 958–67.
26. Mitsudomi T, Yatabe Y. Mutations of the epidermal growth factor receptor gene and related genes as determinants of epidermal growth factor receptor tyrosine kinase inhibitors sensitivity in lung cancer. *Cancer Sci* 2007;98:1817–24.
27. Inoue A, Suzuki T, Fukuhara T, Maemondo M, Kimura Y, Morikawa N, Watanabe H, Saijo Y, Nukiwa T. Prospective phase II study of gefitinib for chemotherapy-naive patients with advanced non-small-cell lung cancer with epidermal growth factor receptor gene mutations. *J Clin Oncol* 2006;24:3340–6.
28. Toyooka S, Kiura K, Mitsudomi T. EGFR mutation and response of lung cancer to gefitinib. *N Engl J Med* 2005;352:2136.
29. Kasahara K, Arao T, Sakai K, Matsumoto K, Sakai A, Kimura H, Sone T, Horiike A, Nishio M, Ohira T, Ikeda N, Yamanaka T, et al. Impact of serum hepatocyte growth factor on treatment response to epidermal growth factor receptor tyrosine kinase inhibitors in patients with non-small cell lung adenocarcinoma. *Clin Cancer Res* 2010;16:4616–24.

Published OnlineFirst January 10, 2011; DOI: 10.1158/1078-0432.CCR-10-1993

Clinical Cancer Research

Transient PI3K Inhibition Induces Apoptosis and Overcomes HGF-Mediated Resistance to EGFR-TKIs in *EGFR* Mutant Lung Cancer

Ivan S. Donev[1], Wei Wang[1], Tadaaki Yamada[1], Qi Li[1], Shinji Takeuchi[1], Kunio Matsumoto[2], Takao Yamori[3], Yasuhiko Nishioka[4], Saburo Sone[4], and Seiji Yano[1]

Abstract

Purpose: Epidermal growth factor receptor (EGFR) tyrosine kinase inhibitors (TKI), such as gefitinib and erlotinib, show favorable response to *EGFR* mutant lung cancer. However, the responders acquire resistance almost without exception. We recently reported that hepatocyte growth factor (HGF) induces EGFR-TKI resistance by activating MET that restores downstream mitogen activated protein kinase (MAPK)/extracellular signal regulated kinase (ERK)1/2 and phosphoinositide 3-kinase (PI3K)/Akt signaling. The purpose of this study was to determine whether inhibition of PI3K, a downstream molecule of both EGFR and MET, could overcome HGF-mediated EGFR-TKI resistance in *EGFR* mutant lung cancer cells PC-9 and HCC827.

Experimental Design: We explored therapeutic effect of a class I PI3K inhibitor PI-103 on HGF-induced EGFR-TKI resistance *in vitro* and *in vivo*.

Results: Unlike gefitinib or erlotinib, continuous exposure with PI-103 inhibited proliferation of PC-9 and HCC827 cells, even in the presence of HGF. On the other hand, in gefitinib-resistant xenograft model by using PC-9 cells mixed with HGF high producing fibroblasts, PI-103 monotherapy did not inhibit tumor growth. However, PI-103 combined with gefitinib successfully regressed gefitinib-resistant tumor. *In vitro* experiments by considering short half-life of PI-103 reveal that transient exposure of PI-103 combined with gefitinib caused sustained inhibition of Akt phosphorylation, but not ERK1/2 phosphorylation, resulting in induction of tumor cell apoptosis even in the presence of HGF.

Conclusions: These results indicate that transient blockade of PI3K/Akt pathway by PI-103 and gefitinib could overcome HGF-mediated resistance to EGFR-TKIs by inducing apoptosis in *EGFR* mutant lung cancer. *Clin Cancer Res; 17(8); 2260–9. ©2011 AACR.*

Introduction

Lung cancer is one of the most prevalent malignancies and the leading cause of cancer-related death worldwide. Non–small cell lung cancer (NSCLC) accounts for nearly 80% of lung cancer cases. Substantial efforts are being made to identify the optimal target for NSCLC therapy. The tyrosine kinase inhibitors (TKI), such as gefitinib and erlotinib, have been shown to inhibit epidermal growth factor receptor (EGFR)-mediated downstream pathways, including mitogen activated protein kinase (MAPK)/extracellular signal regulated kinase (ERK)1/2 and phosphoinositide 3-kinase (PI3K)/Akt, and to show favorable activity in NSCLC patients with mutant *EGFR* (1). Recent phase III clinical trials showed that patients with *EGFR* mutant NSCLC had superior outcomes with gefitinib treatment, compared with standard first-line cytotoxic chemotherapy (2–3). However, the patients develop acquired resistance to EGFR-TKIs almost without exceptions within a couple of years (4). In addition, 20% to 25% patients with *EGFR* activating mutations show intrinsic resistance to EGFR-TKIs.

Two genetically conferred mechanisms–T790M second mutation in *EGFR* (4–5) and the *MET* gene amplification (6)—have been well reported to induce the acquired resistance to EGFR-TKIs in *EGFR* mutant lung cancer. Recently, we identified a third mechanism, hepatocyte growth factor (HGF)-induced resistance. It induces EGFR-TKI resistance by activating MET that restores phosphorylation of downstream MAPK/ERK1/2 and PI3K/Akt pathways (7–8). This is not a genetically conferred mechanism and may be involved in both intrinsic resistance and acquired resistance to EGFR-TKIs in *EGFR* mutant lung cancer (7). Although HGF is reported to be produced predominantly

Authors' Affiliations: [1]Division of Medical Oncology; [2]Division of Tumor Dynamics and Regulation, Cancer Research Institute, Kanazawa University, Kanazawa; [3]Division of Molecular Pharmacology, Cancer Chemotherapy Center, Japanese Foundation for Cancer Research, Tokyo; [4]Department of Respiratory Medicine & Rheumatology, Institute of Health Biosciences, University of Tokushima Graduate School, Tokushima, Japan

Note: Supplementary data for this article are available at Clinical Cancer Research Online (http://clincancerres.aacrjournals.org/).

Corresponding Author: Seiji Yano, Division of Medical Oncology, Cancer Research Institute, Kanazawa University, Kanazawa, Ishikawa 920-0934, Japan. Phone: +81-76-265-2780; Fax: +81-76-234-4524. E-mail: syano@staff.kanazawa-u.ac.jp

doi: 10.1158/1078-0432.CCR-10-1993

Published OnlineFirst January 10, 2011; DOI: 10.1158/1078-0432.CCR-10-1993

Translational Relevance

The acquired resistance to epidermal growth factor receptor (EGFR) tyrosine kinase inhibitors (TKI) is one of the most serious problems on the management of *EGFR* mutant lung cancer. We recently reported the novel mechanism that hepatocyte growth factor (HGF) induces EGFR-TKI resistance by activating MET that restores phosphorylation of downstream mitogen activated protein kinase (MAPK)/extracellular signal regulated kinase (ERK)1/2 and phosphoinositide 3-kinase (PI3K)/Akt pathways.

In this study, we showed that transient blockade of PI3K/Akt pathway by PI3K inhibitor and gefitinib could overcome HGF-mediated resistance to EGFR-TKIs by inducing apoptosis in both *in vitro* and *in vivo* models. Our findings indicate usefulness of double blockade of EGFR and PI3K, and further postulate the need to develop PI3K inhibitor analogues with more suitable pharamcokinetics and metabolic profiles for more successful therapy of *EGFR* mutant lung cancer.

by stromal cells, it can act both autocrine and paracrine fashion when inducing resistance to EGFR-TKIs (7, 9). More recent studies showed that HGF is frequently coexpressed along with the T790M second mutation in *EGFR* (10) and *MET* gene amplification (8) in tumors of patients with acquired resistance to EGFR-TKIs, indicating the importance of HGF as therapeutic target for overcoming resistance to EGFR-TKIs.

Several strategies are available to block HGF-MET–mediated signaling, including ligand (HGF) blockade, MET tyrosine kinase inhibition, and inhibition of downstream molecules (PI3K/Akt, MAPK/ERK; ref. 11). PI3Ks are responsible for the generation of 3-phosphorylated inositides, including the important second messenger PtIns(3,4,5)P3 (antiphosphatidylinositol 3,4,5-triphosphate), resulting in activation of signal transduction pathways in many physiologic process (12). PI3Ks are divided into 3 classes on the basis of their primary structures and *in vitro* substrate specificity (13), with class I PI3Ks being the most well characterized. Class I PI3Ks can be further subdivided into class IA (p110α, p110β, and p110δ) and class IB (p110γ) according to their structure and interaction with p85 and p55 regulatory subunits. Class IA PI3Ks, each composed of a p85 regulatory subunit and a p110 catalytic subunit, are the most widely involved in cancer (14). The major effector of PI3K in cancer is Akt, a serine–threonin kinase that is directly activated in response to PI3K (13–14). Recent studies indicate that the PI3K/Akt pathway plays crucial roles in resistance to various types of TKIs, including EGFR TKIs (6, 15–17). Accordingly, a large numbers of PI3K inhibitors are being developed (18).

We sought to determine whether inhibition of PI3K signaling pathway could overcome EGFR-TKI resistance induced by HGF in *EGFR* mutant lung cancer. We found that transient exposure of class I PI3K inhibitor plus gefitinib was sufficient to overcome HGF-mediated resistance by inducing apoptosis of *EGFR* mutant lung cancer cells.

Materials and Methods

Cell cultures and reagents

The *EGFR* mutant human lung adenocarcinoma cell lines, with exon 19 deletion in *EGFR* PC-9 (del E746_A750) and HCC827 (del E746_A750), were purchased from Immuno-Biological Laboratories Co. and American Type Culture Collection, respectively (19). The H1975 human lung adenocarcinoma cell line with EGFR-L858R/T790M double mutation (20) was kindly provided by Dr. J.D. Minna (University of Texas Southwestern Medical Center, Dallas, TX) and Dr. Y. Sekido (Aichi Cancer Center Research Institute, Nagoya, Japan). Human lung embryonic fibroblasts, MRC-5, were obtained from RIKEN Cell Bank. The PC-9, HCC827, and H1975 cell lines were maintained in RPMI 1640 medium supplemented with 10% FBS and antibiotics. The MRC-5 (p30–p35) was cultured in 10% FBS DMEM (Dulbecco's modied Eagle's medium). All cells were passaged for less than 3 months before renewal from frozen, early-passage stocks obtained from the indicated sources. Cells were regularly screened for mycoplasma with the use of a MycoAlert Mycoplasma Detection Kit (Lonza). Gefitinib, erlotinib, PI-103 (PI3K α inhibitor 1), and GDC-0941 were obtained from AstraZeneca, Chugai Pharmaceutical Co., Calbiochem, and Selleck Chemicals, respectively. Human recombinant HGF was prepared as described previously (21).

Cell proliferation assay

Cell proliferation was measured by the MTT dye reduction method (22). Tumor cells (2×10^3/100 μL per well) were plated into each well of 96-well plates in RPMI 1640 with 10% FBS. After 24 hours incubation, several concentrations of gefitinib, erlotinib, PI-103, and/or HGF were added to each well, and incubation was continued for a further 72 or 48 hours. For short exposure to gefitinib and/or PI-103, tumor cells (8×10^3/800 μL per well) were incubated in 24-well plates. After 24 hours incubation, several concentrations of PI-103 and gefitinib were added for 1 hour, then washed 2 times with PBS, and then replated with fresh medium. Viability was assessed at 48 hours after initial exposure. Cell proliferation was determined with MTT solution (2 mg/mL; Sigma) as described previously (7). Each experiment was done at least 3 times, each with triplicate samples.

Determination of drug synergy

Cells were seeded at a density of 2×10^3 per well of a 96-well plate. Concentration ranges were chosen to span the complete dose-response range of both drugs. All treatments were done in quadruplicate. Cell proliferation/viability was determined after 3 days by using MTT assay. Multiple drug effect analysis was done by using CalcuSyn Software (Biosoft), which quantitatively describes the interaction

Published OnlineFirst January 10, 2011; DOI: 10.1158/1078-0432.CCR-10-1993

between 2 or more drugs (23). This method assigns combination index (CI) values to each drug combination and defines drug synergy when a CI value is less than 1 or drug antagonism when a CI value is greater than 1.

Coculture of lung cancer cells with fibroblasts

Cells were cocultured in transwell chambers separated by 8 μm pore filters. Tumor cells (8×10^3 cells/700 μL) with gefitinib and or PI-103 different doses were placed in the bottom chamber, and fibroblasts (10^4 cells/300 μL) were placed in the top chamber. After 72 hours, the top chamber was removed and cell proliferation was measured by MTT assay. For short exposure to PI-103 and/or gefitinib, the proliferation was assessed after 48 hours and drugs were administered for only 1 hour in different concentration, and then each well was washed twice with PBS and new fresh media were added. Each experiment was done at least 3 times, each with triplicate samples.

Assay for RNA interference

Duplexed Stealth RNAi (Invitrogen) against Akt1-1 (5′-AUACCGGCAAAGAAGCGAUGCUGCA-3′), Akt1-2 (5′-AACCCUCCUUCACAAUAGCCACGUC-3′), and Akt1-3 (5′-UAGCGUGGCCGCCAGGUCUUGAUGU-3′) was used for RNA interference assay. One day before transfection, aliquots of 2×10^4 tumor cells in 400 μL of antibiotic-free medium were plated on 24-well plates. After incubation for 24 hours, the cells were transfected with siRNA (50 pmol) or scramble RNA by using Lipofectamine 2000 (1 μL) in accordance with the manufacturer's instructions. After 24 hours incubation, the cells were washed with PBS and incubated with or without gefitinib (0.1 μmol/L) and/or rhHGF (recombinant human HGF, 20 ng/mL) for an additional 72 hours in antibiotic-containing medium. Cell proliferation was measured by a Cell Counting Kit-8 (Dojin) in accordance with the manufacturer's instructions. Each experiment was done at least in triplicate and 3 times independently.

Xenograft studies in SCID mice

Suspensions of PC-9 cells (5×10^6) with MRC-5 (5×10^6) were injected subcutaneously into the backs of 5-week-old female severe combined immunodeficient mice (SCID). Mice ($n = 6$ per group) were randomized to: (a) control group, (b) gefitinib only (25 mg/kg/d) orally, (c) PI-103 only prepared in 20% 4-hydroxypropyl β-cyclodextrin (5 mg/kg/d) intraperitoneally, or (d) gefitinib (25 mg/kg/d) and PI-103 (5 mg/kg/d). After 4 days (tumors diameter >4 mm), the treatment was started. The tumor volume was calculated (mm^3 = width^2 × length/2). All animal experiments complied with the guidelines for the Institute for Experimental Animals, Advanced Science Research Center, Kanazawa University, Kanazawa, Japan (approval no. AP-081088).

Antibodies and Western blotting

For Western blotting analysis, 40 μg of total protein were resolved by SDS polyacrylamide gel (Bio-Rad) electrophoresis and the proteins were then transferred onto polyvinylidene difluoride membranes (Bio-Rad). After washing 4 times, membranes were incubated with Blocking One (Nacalai Tesque, Inc.) for 1 hour at room temperature and then incubated overnight at 4°C with the following primary antibodies: anti-MET (25H2), anti-phospho-MET (anti-p-MET, Y1234/Y1235; 3D7), anti-p-EGFR (Y1068), anti-ErbB3 (1B2), anti-p-ErbB3 (Tyr1289; 21D3), anti-Akt or p-Akt (Ser473), anti-cleaved caspase-9 (Asp315), anti-cleaved caspase-3 (Asp175), anti-cleaved PARP (Asp214) antibodies (1:1,000 dilution, Cell Signaling Technology), anti-human EGFR (1 μg/mL), anti-human/mouse/rat ERK-1/ERK-2 (0.2 μg/mL), or anti-p-ERK-1/ERK-2 (T202/Y204; 0.1 μg/mL) antibodies (R&D Systems). After washing thrice, membranes were incubated for 1 hour at room temperature with species-specific horseradish peroxidase–conjugated secondary antibodies. Immunoreactive bands were visualized with SuperSignal West Dura Extended Duration Substrate, an enhanced chemiluminescent substrate (Pierce Biotechnology). Each experiment was done at least thrice independently.

TUNEL assay

Terminal deoxynucleotidyl transferase–mediated nick end labeling staining was performed by the Apoptosis Detection System (Promega). Briefly, the frozen tissue sections (9 μm thick) were fixed with PBS containing 4% formalin. The slides were washed with PBS and permeabilized with 0.2% Triton X-100. The samples were then equilibrated, and DNA strand breaks were labeled with fluorescein-12-dUTP (fluorescein-12-2-deoxy-uridine-5-triphosphate) by adding nucleotide mixture and terminal deoxynucleotidyl transferase enzyme. The reaction was stopped with saline sodium citrate, and the localized green fluorescence of apoptotic cells was detected by fluorescence microscopy (×200).

Reverse transcriptase-PCR analysis

Total RNA was isolated from MRC-5 cells treated with various concentration of PI-103 for 24 hours, with ISOGEN RNA extraction. Total RNAs were reversely transcribed by an Omniscript RT Kit (Qiagen) according to the manufacturer's protocols. The primers for HGF and β-actin were as follow: HGF forward, 5′-CAGTGTTGAGAAGTTGAATGC-3′, reverse, 5′-GTGTCATTCATAGTATTGTGAG-3′, and β-actin forward, 5′-AAGAGAGGCATCCTCACCCT-3′, reverse, 5′-TACATGGCTGGGGTGTTGAA-3′. Polymerase chain reaction was done by Ex Taq Hot Start Version (Takara). Cycles for HGF and β-actin were 28 and 26, respectively. The bands were visualized by ethidium bromide staining.

Cell apoptosis assay

Cell apoptosis induced by gefitinib was detected with an Annexin V-FITC Apoptosis Detection Kit I (BD Biosciences Pharmingen) in accordance with the manufacturer's protocols as described previously (7). The analysis was done